14. Banno F, Kaminaka K, Soejima K, Kokame K, Miyata T. Identification of strain-specific variants of mouse Adamts13 gene encoding von Willebrand factor-cleaving protease. J Biol Chem. 2004;279:30896-30903.
15. Zhou W, Bouhassira EE, Tsai HM. An IAP retrotransposon in the mouse ADAMTS13 gene creates ADAMTS13 variant proteins that are less effective in cleaving von Willebrand factor multimers. Blood. 2007;110:886-893.
16. Banno F, Miyata T. Biology of an antithrombotic factor-ADAMTS13. In: Tanaka K, Davie EW, eds. Recent Advances in Thrombosis and Hemostasis. Berlin, Germany: Springer; 2008:162-176.
17. Banno F, Kokame K, Okuda T, et al. Complete deficiency in ADAMTS13 is prothrombotic, but it alone is not sufficient to cause thrombotic thrombocytopenic purpura. Blood. 2006;107:3161-3166.
18. Miyata T, Kokame K, Banno F, Shin Y, Akiyama M. ADAMTS13 assays and ADAMTS13-deficient mice. Curr Opin Hematol. 2007;14:277-283.
19. Kokame K, Matsumoto M, Fujimura Y, Miyata T. VWF73, a region from D1596 to R1668 of von Willebrand factor, provides a minimal substrate for ADAMTS-13. Blood. 2004;103:607-612.
20. Kokame K, Nobe Y, Kokubo Y, Okayama A, Miyata T. FRETS-VWF73, a first fluorogenic substrate for ADAMTS13 assay. Br J Haematol. 2005;129:93-100.
21. Tsuji S, Sugimoto M, Miyata S, Kuwahara M, Kinoshita S, Yoshioka A. Real-time analysis of mural thrombus formation in various platelet aggregation disorders: distinct shear-dependent roles of platelet receptors and adhesive proteins under flow. Blood. 1999;94:968-975.
22. Chauhan AK, Motto DG, Lamb CB, et al. Systemic antithrombotic effects of ADAMTS13. J Exp Med. 2006;203:767-776.
23. Ni H, Denis CV, Subbarao S, et al. Persistence of platelet thrombus formation in arterioles of mice lacking both von Willebrand factor and fibrinogen. J Clin Invest. 2000;106:385-392.
24. Frenette PS, Moyna C, Hartwell DW, Lowe JB, Hynes RO, Wagner DD. Platelet-endothelial interactions in inflamed mesenteric venules. Blood. 1998;91:1318-1324.
25. DiMinno G, Silver MJ. Mouse antithrombotic assay: a simple method for the evaluation of antithrombotic agents in vivo. Potentiation of antithrombotic activity by ethyl alcohol. J Pharmacol Exp Ther. 1983;225:57-60.
26. Jackson SP. The growing complexity of platelet aggregation. Blood. 2007;109:5087-5095.
27. Konstantinides S, Ware J, Marchese P, Almus-Jacobs F, Loskutoff DJ, Ruggeri ZM. Distinct antithrombotic consequences of platelet glycoprotein Ibalpha and VI deficiency in a mouse model of arterial thrombosis. J Thromb Haemost. 2006;4:2014-2021.
28. Shida Y, Nishio K, Sugimoto M, et al. Functional imaging of shear-dependent activity of ADAMTS13 in regulating mural thrombus growth under whole blood flow conditions. Blood. 2008;111:1295-1298.
29. Smyth SS, Reis ED, Vaananen H, Zhang W, Coller BS. Variable protection of beta 3-integrin–deficient mice from thrombosis initiated by different mechanisms. Blood. 2001;98:1055-1062.
30. Cui J, Eitzman DT, Westrick RJ, et al. Spontaneous thrombosis in mice carrying the factor V Leiden mutation. Blood. 2000;96:4222-4226.
31. Weiler H, Lindner V, Kerlin B, et al. Characterization of a mouse model for thrombomodulin deficiency. Arterioscler Thromb Vasc Biol. 2001;21:1531-1537.
32. Suh TT, Holmback K, Jensen NJ, et al. Resolution of spontaneous bleeding events but failure of pregnancy in fibrinogen-deficient mice. Genes Dev. 1995;9:2020-2033.
33. Toomey JR, Kratzer KE, Lasky NM, Broze GJ Jr. Effect of tissue factor deficiency on mouse and tumor development. Proc Natl Acad Sci U S A. 1997;94:6922-6926.
34. Motto DG, Chauhan AK, Zhu G, et al. Shigatoxin triggers thrombotic thrombocytopenic purpura in genetically susceptible ADAMTS13-deficient mice. J Clin Invest. 2005;115:2752-2761.
35. Nishio K, Anderson PJ, Zheng XL, Sadler JE. Binding of platelet glycoprotein Ibalpha to von Willebrand factor domain A1 stimulates the cleavage of the adjacent domain A2 by ADAMTS13. Proc Natl Acad Sci U S A. 2004;101:10578-10583.
36. Shim K, Anderson PJ, Tuley EA, Wiswall E, Sadler JE. Platelet-VWF complexes are preferred substrates of ADAMTS13 under fluid shear stress. Blood. 2008;111:651-657.
37. Donadelli R, Orje JN, Capoferri C, Remuzzi G, Ruggeri ZM. Size regulation of von Willebrand factor-mediated platelet thrombi by ADAMTS13 in flowing blood. Blood. 2006;107:1943-1950.
38. Chauhan AK, Walsh MT, Zhu G, Ginsburg D, Wagner DD, Motto DG. The combined roles of ADAMTS13 and VWF in murine models of TTP, endotoxemia, and thrombosis. Blood. 2008;111:3452-3457.

blood

2009 113: 5039-5040
doi:10.1182/blood-2009-02-201749

ADAMTS13's tail tale

Karen Vanhoorelbeke, Hendrik B. Feys and Simon F. De Meyer

Blood (print ISSN 0006-4971, online ISSN 1528-0020), is published semimonthly by the American Society of Hematology, 1900 M St, NW, Suite 200, Washington DC 20036.

there would be reluctance to advocate long-term primary prophylaxis, this should certainly be offered at times of additional high risk, such as after surgery, immobility, or pregnancy.

Clinically, the issue of thrombophilia testing and management is more relevant in the setting of patients who have experienced an event already. If testing has been performed and high-risk thrombophilia has been identified, this should certainly be taken into account when deciding on extended anticoagulation, especially for spontaneous events. The issue of whether all patients with a DVT should be screened for high-risk thrombophilia is unresolved[7] but, for those with a spontaneous event at a young age and a positive family history, this should be considered. Definition of a positive family history is difficult, but the suggestion offered in this paper of more than 20% of relatives affected is not evidence-based and would be dependent on relatives being available for study.[8]

Any decision on whether to offer long-term anticoagulation will depend on the risk of bleeding while on anticoagulants as well as the thrombotic risk. This study reports a very low annual bleeding risk at 0.29% but with wide confidence intervals, because it is based on only 2 events. The authors speculate that this may be because the thrombophilic defect reduces the bleeding risk, and this observation certainly requires confirmation. Alternative explanations are the young age of the cohort, the fact that the patients are cared for by expert centers, and the small number of events.

Conflict-of-interest disclosure: The author declares no competing financial interests. ■

REFERENCES

1. Egeberg O. Inherited antithrombin deficiency causing thrombophilia. Thromb Diath Haemorrh. 1965;13:516-530.
2. Raffini L. Thrombophilia in children: Who to test, how, when and why? Hematology Am Soc Hematology Educ Program. 2008;2008:228-235.
3. Lijfering WM, Brouwer J-LP, Veeger NJGM, et al. Selective testing for thrombophilia in patients with first venous thrombosis: results from a retrospective family cohort study on absolute thrombotic risk for currently known thrombophilic defects in 2479 relatives. Blood. 2009;113:5314-5322.
4. Lijfering WM, Mudler R, ten Kate MK, et al. Clinical relevance of decreased protein S levels: results from a retrospective family cohort involving 1143 relatives. Blood. 2009;113:1225-1230.
5. Simpson EL, Stevenson MD, Rawdin A, et al. Thrombophilia testing in people with venous thromboembolism: systematic review and cost effectiveness analysis. Health Technology Assessment. 2009;13:1-91.
6. Prandoni P, Lensing AWA, Cogo A, et al. The long term clinical course of acute deep vein thrombosis. Ann Intern Med. 1996;125:1-7.
7. Cohn D, Vansenne F, de Borgie C, et al. Thrombophilia testing for prevention of recurrent venous thromboembolism. Cochrane Database of Systematic Reviews. 2009;1. Art. No.: CD007069. DOI: 10.1002/14651858.CD007069.pub2
8. Cosmi B, Legnani C, Bernardi F, et al. Role of family history in identifying women with thrombophilia and higher risk of venous thromboembolism during oral contraception. Arch Intern Med. 2003;163:1105-1109.

THROMBOSIS & HEMOSTASIS

Comment on Banno et al, page 5323

ADAMTS13's tail tale

Karen Vanhoorelbeke, Hendrik B. Feys, and Simon F. De Meyer KATHOLIEKE UNIVERSITEIT LEUVEN, CAMPUS KORTRIJK

In mice, a long form and a short form of the VWF-cleaving protease ADAMTS13 have been identified, the latter lacking the 4 distal carboxyl-terminal domains. While these are not strictly required for regulating normal size distribution of VWF multimers, in this issue of *Blood*, Banno and colleagues reveal the role of these domains in down-regulating thrombogenesis in vivo.

Since the discovery of ADAMTS13 as a metalloprotease with a multi-domain structure, numerous studies have attempted to shed light on the specific roles of each of the ADAMTS13 domains in digesting large von Willebrand factor (VWF) multimers into smaller, less reactive ones. ADAMTS13 is composed of a signal peptide, propeptide, metalloprotease domain, central TSR (thrombospondin type 1 repeat), Cys-rich region, spacer domain, 7 additional TSRs, and 2 CUB domains. The active site of this enzyme is situated in the metalloprotease domain while the spacer domain plays a crucial role in substrate binding by interacting with a VWF exosite located at the C-terminus of the A2 domain. The exact physiologic significance of the carboxyl-terminal TSRs and the 2 CUB domains still remains unclear, in particular due to the use of different types of in vitro tests, often performed under nonphysiological conditions.

To unravel the in vivo role of the carboxyl-terminal domains of ADAMTS13, Banno and coworkers elegantly take advantage of the presence of 2 kinds of *Adamts13* genes in laboratory mouse strains.[1] The 129/Sv strain has the *Adamts13* gene encoding full-length ADAMTS13 while several other strains, including C57BL/6, harbor an *Adamts13* gene that expresses a truncated form of the enzyme, lacking the 2 C-terminal TSRs and CUB domains due to the insertion of an intracisternal A-particle retrotransposon. By introgressing the C57BL/6-*Adamts13* gene onto the 129/Sv genetic background, the authors generate congenic mice that had the distal C-terminally truncated ADAMTS13 on a 129/Sv genetic background ($Adamts13^{S/S}$) and use wild-type mice that have full-length ADAMTS13 ($Adamts13^{L/L}$) and ADAMTS13$^{-/-}$ mice on the same 129/Sv genetic background for comparison.

The most obvious role of ADAMTS13 is to regulate VWF multimer size. Indeed, ADAMTS13 digests unusually large VWF multimers into smaller less thrombogenic forms,[2] hence preventing the spontaneous intravascular platelet aggregation seen in patients with ADAMTS13 deficiency. Interestingly, Banno et al showed that both $Adamts13^{L/L}$ and $Adamts13^{S/S}$ mice do not have ultra large VWF multimers in their plasma, implying that the C-terminal domains are not strictly needed for maintaining normal VWF size. Consequently, the 2 C-terminal TSRS and CUB domains are not essential for the removal of ultralarge VWF multimers from the plasma.

Following VWF size regulation, a fascinating role of ADAMTS13 in attenuating thrombus growth has been described, possibly by cleaving VWF multimers that are peripheral to or incorporated in platelet rich thrombi.[3] In this study, Banno et al used the congenic mice to demonstrate that the 2 C-terminal TSRs and CUB domains play a role in the down-regulation of thrombogenesis under high shear conditions. Both in vitro flow chamber experiments at high shear rates and in vivo thrombosis models show that blood from $Adamts13^{S/S}$ mice is more thrombogenic. This is evidenced by accelerated thrombus formation and decreased time to occlusion respectively when compared with blood from $Adamts13^{L/L}$ mice. Whether this would

translate into an increased risk of thrombosis in patients having comparable truncated forms of ADAMTS13 remains elusive.

In this article, Banno et al provide the first in vivo insights on the physiological significance of the distal carboxyl-terminal domains of ADAMTS13. The exact mechanism of thrombus size attenuation by ADAMTS13 and, in particular, the specific involvement of the carboxyl-terminal domains still remains to be determined. Does ADAMTS13 digest VWF multimers on the surface of the platelet thrombus or is thrombus size attenuation by ADAMTS13 independent of its VWF-cleaving activity? In this context, it is certainly intriguing that the mechanism of VWF size regulation by ADAMTS13 might be different from that of VWF processing during thrombus growth. Clearly, these new findings provide another impetus in the quest to understand the structure-function relationship of ADAMTS13. Obviously, this is not the end of the tale.

Conflict-of-interest disclosure: The authors declare no competing financial interests. ■

REFERENCES

1. Banno F, Chauhan A, Kokame K, et al. The distal carboxyl-terminal domains of ADAMTS13 are required for regulation of in vivo thrombus formation. Blood. 2009;113:5323-5329.

2. Dong JF, Moake JL, Nolasco L, et al. ADAMTS-13 rapidly cleaves newly secreted ultralarge von Willebrand factor multimers on the endothelial surface under flowing conditions. Blood. 2002;100:4033-4039.

3. Chauhan AK, Motto DG, Lamb CB, et al. Systemic antithrombotic effects of ADAMTS13. J Exp Med. 2006;203:767-776.

● ● ● TRANSPLANTATION

Comment on Kamei et al, page 5041

Scanning for the origins of mHags

John A. Hansen FRED HUTCHINSON CANCER RESEARCH CENTER

In this issue of *Blood*, Kamei and colleagues introduce an innovative approach for identifying the genes that encode novel T cell–defined human minor histocompatibility antigens (mHags). In this significant methodologic advance, they demonstrate how the rich human genetic variation data generated for the International Human HapMap Project, together with the available HapMap B-lymphoblastoid cell lines that have undergone extensive genome-wide sequencing, can be used to identify the functional genetic variants responsible for the cellular peptides recognized by selected T-cell clones.

Human minor histocompatibility antigens (mHags) have been recognized as barriers to successful hematopoietic cell transplantation (HCT) from normal donors for more than 30 years.[1] Success following HCT is ultimately determined by the ability to achieve sustained engraftment, eradication of abnormal or malignant host cells, and control of graft-versus-host disease (GVHD). Each of these clinical end points is influenced by the nature and extent of the genetic disparity between donor and recipient. Graft rejection and GVHD are immune-mediated reactions induced by histocompatibility differences between donor and recipient. GVHD occurs when immune-competent donor T cells are transplanted to an immune-compromised host, and the incompatibility between donor and recipient is sufficient to induce T-cell activation.[2] The histocompatibility differences responsible for these T-cell responses are encoded by polymorphic genes located throughout the genome. T-cell recognition of these differences can occur only when the variant peptide in a recipient is foreign to the donor and is appropriately processed and presented at the cell surface by the HLA alleles of the recipient. Polymorphic peptides fulfilling these requirements are called mHags.[1,3]

Although severe GVHD has an adverse effect on morbidity and mortality, occurrence of GVHD is also associated with lower relapse rates, demonstrating that host reactivity of donor T cells can also mediate a significant graft-versus-leukemia (GVL) effect and thereby directly contributes to the curative potential of allogeneic HCT for patients with hematologic malignancy. The GVL effect has become an important model system for exploring new strategies aimed at improving the antitumor potential of T cell–based immunotherapy. These efforts have largely focused on understanding the mechanisms of GVL and the identification of the molecules that could be the potential targets for T-cell immunotherapy.[4,5] Improved techniques for cloning mHag-specific T cells and eluting candidate peptides from major histocompatibility complex molecules in the late 1980s made possible the initial identification of individual mHags. However, the process was difficult, and progress in expanding the library of well-characterized mHags has been slow.

In this issue of *Blood*, Kamei et al introduce a novel approach for identifying T cell–defined mHag loci using publically available resources generated by the International HapMap Project and including the B-lymphoblastoid cell lines that were the source of DNA sequenced for the HapMap project and the resulting large dataset of sequence-based genotypes.[6-8] These cell lines are publicly available, and once they have been transduced with the appropriate HLA restriction element, they can be tested as targets to determine whether they contain the DNA sequence necessary to encode specific T cell–defined peptides. Mapping of the gene encoding the mHag is accomplished by combining the results of immune-based functional assays with a whole genome association analysis by scanning the known sequence polymorphisms (SNPs) in the vast HapMap database, which currently consists of more than 3 million genetic markers expressed by these reference cell lines. The power and resolution of genetic mapping obtainable with this resource will continue to expand in the future as the numbers of new reference samples sequenced increases, and the racial diversity of the reference panel is broadened. The approach described here by Kamei et al should contribute substantially to the development of a more comprehensive and efficient characterization of mHags. This method may also prove useful for the genetic mapping of other genetic traits.

Conflict-of-interest disclosure: The author declares no competing financial interests. ■

REFERENCES

1. Snell GD, Dausset J, Nathenson S. Histocompatibility. New York, NY: Academic Press; 1976.

2. Elkins WL. Cellular immunology and the pathogenesis of graft versus host reactions (review). Prog Allergy. 1971;15:78-187.

3. Perreault C, Décary F, Brochu S, et al. Minor histocompatibility antigens. Blood. 1990;76:1269-1280.

4. Bleakley M, Riddell SR. Molecules and mechanisms of the graft-versus-leukaemia effect. Nat Rev Cancer. 2004;4:371-380.

5. Spierings E, Goulmy E. Expanding the immunotherapeutic potential of minor histocompatibility antigens. J Clin Invest. 2005;115:3397-3400.

6. Kamei M, Nannya Y, Torikai H, et al. HapMap scanning of novel human minor histocompatibility antigens. Blood. 2009;113:5041-5048.

7. The International HapMap Consortium. The International HapMap Project. Nature. 2003;426:789-796.

8. Frazer KA, Ballinger DG, Cox DR, et al. A second generation human haplotype map of over 3.1 million SNPs. Nature. 2007;449:851-861.

Brief report

ADAMTS13 gene deletion aggravates ischemic brain damage: a possible neuroprotective role of ADAMTS13 by ameliorating postischemic hypoperfusion

*Masayuki Fujioka,[1-3] *Kazuhide Hayakawa,[2] Kenichi Mishima,[2] Ai Kunizawa,[3] Keiichi Irie,[2] Sei Higuchi,[2] Takafumi Nakano,[2] Carl Muroi,[3] Hidetada Fukushima,[1] Mitsuhiko Sugimoto,[4] Fumiaki Banno,[5] Koichi Kokame,[5] Toshiyuki Miyata,[5] Michihiro Fujiwara,[2] Kazuo Okuchi,[1] and Kenji Nishio[1]

[1]Department of Emergency and Critical Care Medicine, Nara Medical University, Nara, Japan; [2]Department of Neuropharmacology, Faculty of Pharmaceutical Sciences, Fukuoka University, Fukuoka, Japan; [3]Stroke Center, Helios General Hosp Aue, Dresden University of Technology, Saxony, Germany; [4]Department of Regulatory Medicine for Thrombosis, Nara Medical University, Nara, Japan; and [5]Research Institute, National Cardiovascular Center, Suita, Japan

Reperfusion after brain ischemia causes thrombus formation and microcirculatory disturbances, which are dependent on the platelet glycoprotein Ib–von Willebrand factor (VWF) axis. Because ADAMTS13 cleaves VWF and limits platelet-dependent thrombus growth, ADAMTS13 may ameliorate ischemic brain damage in acute stroke. We investigated the effects of ADAMTS13 on ischemia-reperfusion injury using a 30-minute middle cerebral artery occlusion model in *Adamts13*$^{-/-}$ and wild-type mice. After reperfusion for 0.5 hours, the regional cerebral blood flow in the ischemic cortex was decreased markedly in *Adamts13*$^{-/-}$ mice compared with wild-type mice ($P < .05$), which also resulted in a larger infarct volume after 24 hours for *Adamts13*$^{-/-}$ compared with wild-type mice ($P < .01$). Thus, *Adamts13* gene deletion aggravated ischemic brain damage, suggesting that ADAMTS13 may protect the brain from ischemia by regulating VWF-platelet interactions after reperfusion. These results indicate that ADAMTS13 may be a useful therapeutic agent for stroke. (Blood. 2010; 115:1650-1653)

Introduction

von Willebrand factor (VWF) is a large multimeric protein that plays a key role in thrombus formation by tethering platelets at sites of vascular injury.[1] Smaller VWF multimers are less active, and the potent thrombogenic activity of ultra-large VWF (ULVWF) secreted from endothelium is regulated in vivo through cleavage by ADAMTS13.[2,3] The importance of this mechanism for normal hemostasis is supported by evidence that patients with deficiency of ADAMTS13 function, diagnosed with thrombotic thrombocytopenic purpura, have ULVWF in circulating blood and VWF-dependent microvascular thrombosis.[2] Recently, we demonstrated that ADAMTS13 cleaves VWF on the surface of platelet thrombi in a shear force–dependent manner, which limits thrombus growth in vitro.[4] These data suggest that ADAMTS13 is a key molecule that maintains a physiologic balance between hemostasis and thrombosis through regulation of VWF function in vivo.

ADAMTS13 function is crucial for preventing thrombosis in the cerebral microvasculature, as indicated by the occurrence of neurologic deficits in thrombotic thrombocytopenic purpura, but the role of ADMTS13 in the pathogenesis of reperfusion injury after arterial thrombosis has not been established. To address this issue, we investigated the role of ADAMTS13 in a transient middle cerebral arterial occlusion (MCAO) model of ischemia-reperfusion injury in the mouse brain[5] using *Adamts*$^{-/-}$ mice.[6]

Because brain ischemia-reperfusion injury is dependent on the platelet glycoprotein Ib–VWF axis[7] and platelet thrombosis adversely affects the postischemic cerebral microcirculation[8-11] leading to secondary brain damage,[10] ADAMTS13 may reduce platelet thrombus growth and thereby ameliorate ischemic brain injury by improving the postischemic no-reflow phenomenon.[12] Here we demonstrate that *Adamts13* gene deletion aggravates postischemic cerebral blood reflow, resulting in larger infarct volume. This result suggests that ADAMTS13 may indeed suppress excessive platelet thrombus growth in vivo.

Methods

The effect of *Adamts13* gene deletion on brain ischemia was studied using male *Adamts13*$^{-/-}$ (−/−) mice and wild-type (+/+) mice generated by our study group.[6] We used male mice only to obtain consistent results because female mice are known to be more resistant to stroke. The experimenters were blinded to the genotype of each animal until all studies had been finished. This study was approved by the institutional ethics committee of Fukuoka University.

Transient MCAO

Focal cerebral ischemia (MCAO by intraluminal thread) was induced in *Adamts13*$^{-/-}$ and wild-type mice as previously described.[5,13,14] Preliminary experiments using 1-hour MCAO gave excessively high mortality of 4 of 5 for one group and 1 of 4 for another. Therefore, we reduced the time of MCAO to 30 minutes. Body temperature was maintained at 36.5°C to 37.0°C during surgery. The success of the left MCAO was confirmed according to the following criteria: (1) regional cerebral blood flow (rCBF)

Submitted June 29, 2009; accepted October 20, 2009. Prepublished online as *Blood* First Edition paper, November 13, 2009; DOI 10.1182/blood-2009-06-230110.

*M. Fujioka and K.H. contributed equally to this study.

This study was presented in part at the 50th Annual Meeting of the American Society of Hematology, San Francisco, CA, December 6-9, 2008.

An Inside *Blood* analysis of this article appears at the front of this issue.

The publication costs of this article were defrayed in part by page charge payment. Therefore, and solely to indicate this fact, this article is hereby marked "advertisement" in accordance with 18 USC section 1734.

in the left cerebral cortex at the thread insertion less than 20% of pre-MCAO rCBF; and (2) consistent presence of significant ischemic neurologic symptoms of the left cerebral hemisphere, including right forepaw paralysis and right circling behavior during 30-minute MCAO.

rCBF

The rCBF was measured by LASER Doppler flowmetry (LDF; ALF21, Advance Co) as previously described.[5] The LDF probe was placed in the left cerebral cortex stereotaxically. The rCBF was monitored in all animals during the period between 30 minutes before MCAO and immediately after reperfusion.

Cerebral infarct volume and histology 24 hours after MCAO

The brains were sectioned coronally (four 2-mm-thick slices) according to a mouse brain matrix 24 hours after MCAO or sham operation. The infarct area was measured using an image-analysis system (National Institutes of Health Image software, Version 1.63) in each slice stained with 2,3,5 triphenyltetrazolium chloride, and the infarct volume was calculated.[5,13] Paraffin-embedded brains were stained with phosphotungstic acid hematoxylin (PTAH) to demonstrate fibrin in thrombi or incubated with anti-VWF antibody (sc-8068; Santa Cruz Biotechnology), followed by a standard avidin-biotin-peroxidase complex technique to demonstrate VWF in thrombi.

Neurologic assessment

Neurologic deficit was assessed at 24 hours after MCAO using a neurologic score as previously described,[13] and the survival rates were also measured at 24 hours after MCAO.

Statistical analysis

Data are mean plus or minus SEM. For multiple pairwise comparisons, 2-way analysis of variance followed by Scheffé test was performed. When only 2 groups were compared, Student *t* test was used. Probability values less than .05 were considered to be of statistical significance.

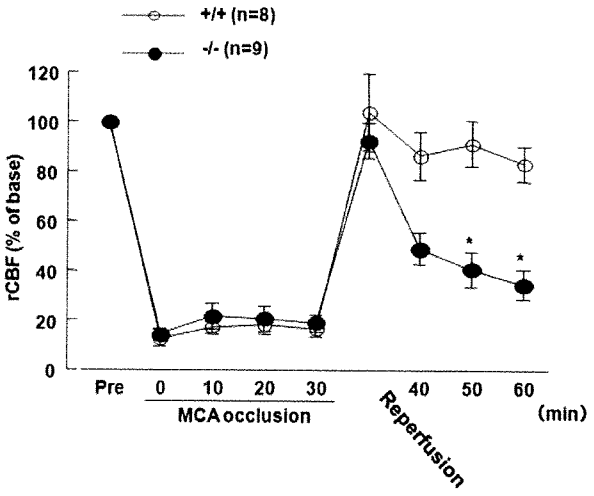

Figure 1. Effect of *Adamts13* gene deletion on rCBF in mice of 30-minute MCAO model. Male *Adamts13*$^{-/-}$ (−/−) mice and wild-type (+/+) mice in an SV129-genetic background were used to study the effect of ADAMTS13 deficiency on brain ischemia: −/− (n = 25) and +/+ (n = 25) mice (8-10 weeks of age, 20-23 g of body weight). The focal cerebral ischemia (30-minute MCAO by intraluminal thread) was induced in the −/− (n = 20) and +/+ (n = 20) mice as previously described (sham surgery in −/−, n = 5; and +/+, n = 5). This study was approved by the institutional ethics committee at Nara Medical University. The rCBF was measured by LDF (ALF21; Advance Co). The rCBF was recorded over time (immediately before and after MCAO; 10, 20, and 30 minutes after MCAO; immediately after reperfusion; and 10, 20, and 30 minutes after reperfusion). The rCBFs during occlusion and reperfusion were expressed as a percentage of the baseline LDF value. The rCBF decreased to less than 20% of the baseline value during 30 minutes of MCAO and returned to the baseline immediately after reperfusion in both −/− and WT mice. The rCBF in −/− mice, however, progressively decreased more markedly compared with that in +/+ after reperfusion (percentage rCBF: −/−, n = 9, vs +/+, n = 8, at 20 and 30 minutes after reperfusion; 40.8 ± 7.1 vs 91.4 ± 9.1, and 34.6 ± 5.8 vs 83.2 ± 6.8, respectively). *$P < .05$ vs WT, Scheffé test after 2-way repeated-measures analysis of variance ($F(8,134) = 6.668$, $P < .01$). Values are mean ± SEM.

Results and discussion

The rCBF decreased to less than 20% of the baseline value during 30-minute MCAO and returned to baseline immediately after reperfusion in both *Adamts13*$^{-/-}$ and wild-type mice. However, during the subsequent 30 minutes, the rCBF for both groups decreased, suggesting that ischemia-reperfusion had induced thrombosis. The rCBF for *Adamts13*$^{-/-}$ mice progressively decreased compared with wild-type mice (significantly decreased at 20 and 30 minutes after reperfusion, $P < .05$, Scheffé test, Figure 1).

The survival rates of the *Adamts13*$^{-/-}$ and wild-type mice did not differ (17 of 20 vs 16 of 20, respectively). However, *Adamts13*$^{-/-}$ mice had larger brain infarctions compared with wild-type mice 24 hours after MCAO ($P < .01$; Figure 2A), which is reflected by a difference in neurologic score assessing left hemisphere function (Figure 2B). Histologic and immunohistochemical examinations revealed that more thrombi containing fibrin and VWF were observed in *Adamts13*$^{-/-}$ mice (Figure 2C), which may contribute to the lowered rCBF and increased infarct volume in *Adamts13*$^{-/-}$ mice. These results indicate that *Adamts13* gene deletion aggravates ischemic brain damage.

Our results indicate that ADAMTS13 is crucial in vivo to protect the brain from ischemia-reperfusion injury by ameliorating postischemic hypoperfusion. The possible neuroprotective effect of ADAMTS13 may result from the cleavage of ULVWF secreted from endothelium activated by ischemia[3,15] and cleavage of VWF multimers on the surface of thrombi formed on the ischemic endothelial cells.[4] Without adequate ADAMTS13, progressive platelet thrombus growth may narrow the microvascular lumen, increasing fluid shear stress locally. Without negative feedback regulation by proteolysis of VWF, ischemia-reperfusion injury may cause a vicious cycle in which the VWF-platelet thrombosis and fluid shear stress enhance each other and contribute to the progressive deterioration of cerebral blood reflow, as observed in the *Adamts13*$^{-/-}$ mice. ADAMTS13 may, therefore, prevent microvascular occlusion under high shear stress and augment the cerebral blood flow after ischemia-reperfusion in vivo.

In addition to VWF-platelet thrombus formation,[10,11,16,17] microvascular plugging by activated leukocytes[18-20] can lead to no-reflow phenomena in brain ischemia.[11] Importantly, platelet-ULVWF strings support leukocyte tethering on the endothelium under high fluid-shear stress.[21,22] A recent study suggested that deficiency of ADAMTS13 can increase leukocyte adhesion on the vessels and extravasation.[23] Thus, ADAMTS13 deficiency may enhance the leukocyte activation in the ischemic cerebral vasculature after reperfusion and thereby aggravate ischemic brain damage. Indeed, *Adamts13*$^{-/-}$ mice accumulated more inflammatory cells in the brain tissue than wild-type mice after MCAO (Figure 2C), suggesting that ADAMTS13 may reduce inflammation as well as thrombosis associated with ischemia-reperfusion injury.

In conclusion, ADAMTS13 deficiency causes progressive decline of postischemic rCBF, with a resultant exacerbation of ischemic brain injury, suggesting an important role of ADAMTS13 in neuroprotection. The regulation of VWF-platelet interactions by supplementation with ADAMTS13 may ameliorate ischemia-reperfusion injury of the brain. Because ADAMTS13 tends to

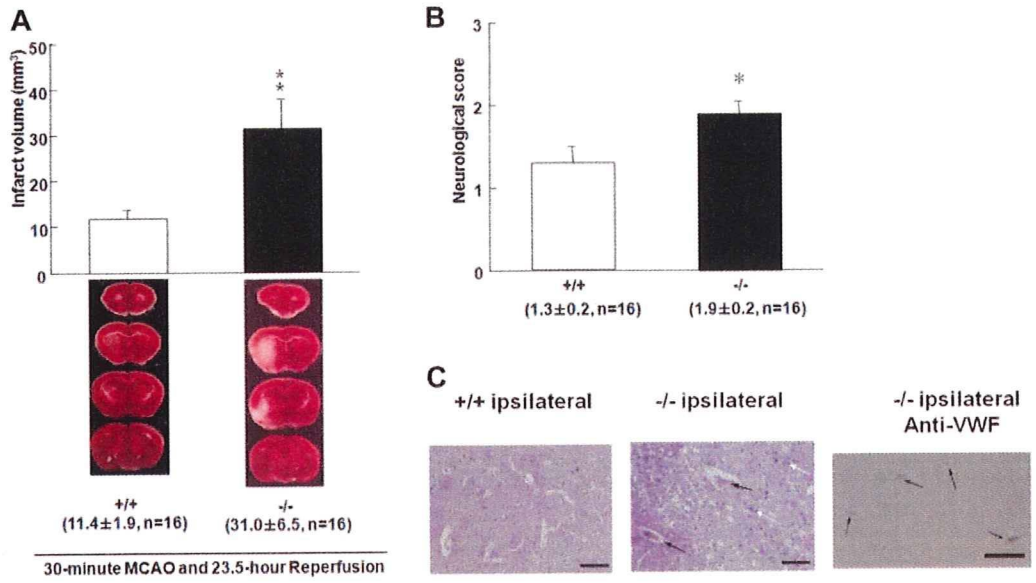

Figure 2. Effect of *Adamts13* gene deletion on brain infarct in mice after 30-minute MCAO. (A) These are coronal sections through the brain in both groups stained with 2,3,5 triphenyltetrazolium chloride. Red areas represent vital brain tissue, and white areas represent cerebral infarction. *Adamts13*$^{-/-}$ ($-/-$) mice had significantly larger volume of brain infarct compared with wild-type ($+/+$) mice after 23.5-hour reperfusion after 30-minute MCAO ($-/-$, n = 16, vs $+/+$, n = 16, $^{**}P < .01$, Student *t* test). Values are mean ± SEM (mm^3). The average infarct volume was 31.0 ± 6.5 mm^3 for ADAMTS13 $^{-/-}$ mice and 11.4 ± 1.9 mm^3 for $+/+$ mice. The survival rates of the $-/-$ and $+/+$ mice did not differ (17 of 20 vs 16 of 20, respectively). No ischemic change was observed in the brain of $-/-$ and $+/+$ mice after sham operation. (B) Neurologic score was measured 24 hours after MCAO. Neurologic scores were measured from the point according to the neurologic findings as follows: 0 indicates normal motor function; 1, flexion of torso and of contralateral forelimb on lifting of the animal by the tail; 2, circling to the ipsilateral side but normal posture at rest; 3, circling to the ipsilateral side; 4, rolling to the ipsilateral side; and 5, leaning to the ipsilateral side at rest (no spontaneous motor activity). $^{*}P < .05$. (C) Representative PTAH-stained sections of infarct area for wild-type ($+/+$) and *Adamts13*$^{-/-}$ ($-/-$) mice. There were more thrombi and inflammatory cells in the lesions of *Adamts13*$^{-/-}$ mice compared with $+/+$ mice (black arrows represent thrombus; white arrow, inflammatory cells infiltration). The area comparable with PTAH staining for $-/-$ mice was immunostained using anti-VWF antibody. VWF is detected in thrombi as brown staining ($-/-$ ipsilateral anti-VWF). Images were generated using an Olympus BH-2 microscope with an Olympus DP20-5 digital camera (original magnification ×200). Bar represents 40 μm.

dissolve excessive VWF-platelet thrombi with increasing efficiency as the flow path narrows, treatment of acute ischemic stroke with ADAMTS13 might have a relatively low risk of hemorrhagic complications.

Note added in proof. After submission of our paper, the complementary paper by Zhao et al[24] appeared in *Blood*, which also demonstrated the important role of ADAMTS13 for brain reperfusion injury.

Acknowledgments

The authors thank Dr Kouko Tatsumi and Dr Takahiko Kasai at the Laboratory of the Department of Anatomy and Neuroscience, and Diagnostic Pathology, respectively, in Nara Medical University, for histologic assistance.

Authorship

Contribution: M. Fujioka and K.H. performed most of the animal experiments and prepared the manuscript; A.K., K.I., S.H., T.N., and C.M. helped to perform the animal experiments; H.F. and M.S. worked on the experimental design and data analysis; K.M., M. Fujiwara, K.O., and K.N. provided direction throughout the work, made the overall experimental design, and edited the manuscript; and F.B., K.K., and T.M. produced the ADAMTS13 gene-deleted mice.

Conflict-of-interest disclosure: The authors declare no competing financial interests.

Correspondence: Kenji Nishio, Department of Emergency and Critical Care Medicine, Nara Medical University, 840 Shijo-cho, Kashihara, Nara 634-8522, Japan; e-mail: knishio@naramed-u.ac.jp.

References

1. Ruggeri ZM. Von Willebrand factor, platelets and endothelial cell interactions. *J Thromb Haemost.* 2003;1(7):1335-1342.
2. Sadler JE. Von Willebrand factor, ADAMTS13, and thrombotic thrombocytopenic purpura. *Blood.* 2008;112(1):11-18.
3. Dong JF, Moake JL, Nolasco L, et al. ADAMTS-13 rapidly cleaves newly secreted ultralarge von Willebrand factor multimers on the endothelial surface under flowing conditions. *Blood.* 2002; 100(12):4033-4039.
4. Shida Y, Nishio K, Sugimoto M, et al. Functional imaging of shear-dependent activity of ADAMTS13 in regulating mural thrombus growth under whole blood flow conditions. *Blood.* 2008; 111(3):1295-1298.
5. Hayakawa K, Mishima K, Nozako M, et al. Delayed treatment with cannabidiol has a cerebroprotective action via a cannabinoid receptor-independent myeloperoxidase-inhibiting mechanism. *J Neurochem.* 2007;102(5):1488-1496.
6. Banno F, Kokame K, Okuda T, et al. Complete deficiency in ADAMTS13 is prothrombotic, but it alone is not sufficient to cause thrombotic thrombocytopenic purpura. *Blood.* 2006;107(8):3161-3166.
7. Kleinschnitz C, De Meyer SF, Schwarz T, et al. Deficiency of von Willebrand factor protects mice from ischemic stroke. *Blood.* 2009;113(15):3600-3603.
8. Stoll G, Kleinschnitz C, Nieswandt B. Molecular mechanisms of thrombus formation in ischemic stroke: novel insights and targets for treatment. *Blood.* 2008;112(9):3555-3562.
9. Kochanek PM, Dutka AJ, Kumaroo KK, Hallenbeck JM. Effects of prostacyclin, indomethacin, and heparin on cerebral blood flow and platelet adhesion after multifocal ischemia of canine brain. *Stroke.* 1988;19(6):693-699.

10. Lo EH, Dalkara T, Moskowitz MA. Mechanisms, challenges and opportunities in stroke. *Nat Rev Neurosci.* 2003;4(5):399-415.
11. del Zoppo GJ, Mabuchi T. Cerebral microvessel responses to focal ischemia. *J Cereb Blood Flow Metab.* 2003;23(8):879-894.
12. Ames A 3rd, Wright RL, Kowada M, Thurston JM, Majno G. Cerebral ischemia: II. the no-reflow phenomenon. *Am J Pathol.* 1968;52(2):437-453.
13. Hayakawa K, Mishima K, Nozako M, et al. Delayed treatment with minocycline ameliorates neurologic impairment through activated microglia expressing a high-mobility group box1-inhibiting mechanism. *Stroke.* 2008;39(3):951-958.
14. Limbourg FP, Huang Z, Plumier JC, et al. Rapid nontranscriptional activation of endothelial nitric oxide synthase mediates increased cerebral blood flow and stroke protection by corticosteroids. *J Clin Invest.* 2002;110(11):1729-1738.
15. Huang J, Roth R, Heuser JE, Sadler JE. Integrin alpha(v)beta(3) on human endothelial cells binds von Willebrand factor strings under fluid shear stress. *Blood.* 2009;113(7):1589-1597.
16. Kleinschnitz C, Stoll G, Bendszus M, et al. Targeting coagulation factor XII provides protection from pathological thrombosis in cerebral ischemia without interfering with hemostasis. *J Exp Med.* 2006;203(3):513-518.
17. Kleinschnitz C, Pozgajova M, Pham M, Bendszus M, Nieswandt B, Stoll G. Targeting platelets in acute experimental stroke: impact of glycoprotein Ib, VI, and IIb/IIIa blockade on infarct size, functional outcome, and intracranial bleeding. *Circulation.* 2007;115(17):2323-2330.
18. Ishikawa M, Cooper D, Arumugam TV, Zhang JH, Nanda A, Granger DN. Platelet-leukocyte-endothelial cell interactions after middle cerebral artery occlusion and reperfusion. *J Cereb Blood Flow Metab.* 2004;24(8):907-915.
19. Connolly ES Jr, Winfree CJ, Springer TA, et al. Cerebral protection in homozygous null ICAM-1 mice after middle cerebral artery occlusion: role of neutrophil adhesion in the pathogenesis of stroke. *J Clin Invest.* 1996;97(1):209-216.
20. Mori E, del Zoppo GJ, Chambers JD, Copeland BR, Arfors KE. Inhibition of polymorphonuclear leukocyte adherence suppresses no-reflow after focal cerebral ischemia in baboons. *Stroke.* 1992;23(5):712-718.
21. Bernardo A, Ball C, Nolasco L, Choi H, Moake JL, Dong JF. Platelets adhered to endothelial cell-bound ultra-large von Willebrand factor strings support leukocyte tethering and rolling under high shear stress. *J Thromb Haemost.* 2005;3(3):562-570.
22. Pendu R, Terraube V, Christophe OD, et al. P-selectin glycoprotein ligand 1 and beta2-integrins cooperate in the adhesion of leukocytes to von Willebrand factor. *Blood.* 2006;108(12):3746-3752.
23. Chauhan AK, Kisucka J, Brill A, Walsh MT, Scheiflinger F, Wagner DD. ADAMTS13: a new link between thrombosis and inflammation. *J Exp Med.* 2008;205(9):2065-2074.
24. Zhao BQ, Chauhan AK, Canault M, et al. von Willebrand factor-cleaving protease ADAMTS13 reduces ischemic brain injury in experimental stroke. *Blood.* 2009;114(15):3329-3334.

Int J Hematol (2010) 91:30–35
DOI 10.1007/s12185-009-0477-0

The function of ADAMTS13 in thrombogenesis in vivo: insights from mutant mice

Fumiaki Banno · Anil K. Chauhan · Toshiyuki Miyata

Received: 31 August 2009 / Accepted: 16 December 2009 / Published online: 5 January 2010

Abstract Recently, two independent groups have established ADAMTS13-deficient mice using gene-targeting techniques. In humans, genetic or acquired deficiency in ADAMTS13 leads to a potentially fatal syndrome, thrombotic thrombocytopenic purpura (TTP). Surprisingly, ADAMTS13-deficient mice are viable with no apparent signs of TTP. However, these mouse models indicate that ADAMTS13 down-regulates platelet adhesion and aggregation in vivo, and ADAMTS13 deficiency can provide enhanced thrombus formation at the site of vascular lesions. In addition, ADAMTS13 by cleaving hyperactive ultra-large von Willebrand factor multimers not only down-regulates thrombosis but also inflammation. ADAMTS13-congenic mice that carry a truncated form of ADAMTS13 lacking the C-terminal domains have also been developed. Phenotypes of the congenic mice indicate the physiological significance of the C-terminal domains of ADAMTS13 in down-regulating thrombus growth. The studies mentioned here in different mouse models uncover the in vivo function of ADAMTS13 and strengthened the understanding of the mechanism of systemic disease TTP.

F. Banno · T. Miyata (✉)
National Cardiovascular Center Research Institute,
5-7-1 Fujishirodai, Suita, Osaka 565-8565, Japan
e-mail: miyata@ri.ncvc.go.jp

F. Banno
e-mail: banno@ri.ncvc.go.jp

A. K. Chauhan
Department of Internal Medicine,
University of Iowa Carver College of Medicine,
500 Newton Road, Iowa, IA 52242, USA
e-mail: anil-chauhan@uiowa.edu

Keywords ADAMTS13 · von Willebrand factor · ADAMTS13-deficient mice · ADAMTS13-congenic mice · Thrombosis · Inflammation

1 Introduction

ADAMTS13 is a plasma protease that cleaves von Willebrand factor (VWF) [1]. VWF is a large protein that circulates in blood as homomultimers of varied sizes. One of main functions of VWF is to mediate adhesion between platelets and between platelets and vascular subendothelium. Both types of adhesion are essential to maintain the balance between hemorrhage and thrombosis. The adhesive activity of VWF depends on its molecular sizes and, in particular, ultra-large VWF (UL-VWF) multimers exceeding 20,000 kDa can form high strength bonds with platelet GPIbα and induce excessive platelet aggregation under shear stress. UL-VWF multimers are normally cleaved by ADAMTS13 to smaller forms, thus restraining spontaneous platelet thrombus formation. The lack of ADAMTS13 activity allows UL-VWF multimers to persist in the circulation and leads to the development of thrombotic thrombocytopenic purpura (TTP) [1].

TTP is a serious systemic disease caused by excessive aggregation of platelets and VWF in small vessels of many organs. The accumulated platelet thrombi obstruct blood flow and cause consumptive thrombocytopenia, fragmentation of red blood cells with anemia, renal and cerebral failure, and fever. Without treatment, the mortality rate of affected patients exceeds 90%, but plasma exchange reduces the death rate to approximately 20%. The discovery of ADAMTS13 as VWF-cleaving protease increases our understanding of TTP pathophysiology. Congenital TTP (Upshaw-Schulman syndrome) is associated with the ADAMTS13 gene mutations.

Some forms of acquired TTP (e.g., idiopathic TTP, ticlopidine-induced TTP) are associated with the production of autoantibodies against ADAMTS13.

Recently, murine models of ADAMTS13 deficiency have been developed by gene-targeting technique by two independent groups [2, 3]. Models resulting from a naturally occurring mutation have also been established [4]. These animal models have proven useful to elucidate ADAMTS13 functions in vivo and the pathophysiology of TTP. This review summarizes phenotypic characteristics of *Adamts13*-mutant mice, focusing on roles of ADAMTS13 in thrombosis, endotoxemia and inflammation.

2 The gene structure of mouse *Adamts13*

In mice, two kinds of *Adamts13* gene are present in a strain-specific manner (Fig. 1) [5]. The *Adamts13* gene of the 129/Sv, FVB/NJ, and CAST/EiJ strains contains 29 exons like the human *ADAMTS13* gene and encodes ADAMTS13 protein with the same domain constitutions as human ADAMTS13, designated as ADAMTS13-L. On the other hand, several strains of mice, including the BALB/c, C3H/He, C57BL/6, and DBA/2 strains, harbor the insertion of an intracisternal A-particle (IAP) retrotransposon into intron 23 of the *Adamts13* gene. The inserted IAP is one of the endogenous transposable elements present at approximately 2,000 sites in the mouse genome. Like retroviruses, the IAP contains two long terminal repeats with signals for the initiation and regulation of transcription and for the polyadenylation of transcripts. The IAP insertion into the *Adamts13* gene produces a cryptic splicing site followed by a premature in-frame stop codon and a polyadenylation signal derived from the long terminal repeat. As a result, ADAMTS13 protein that lacks the C-terminal two thrombospondin type 1

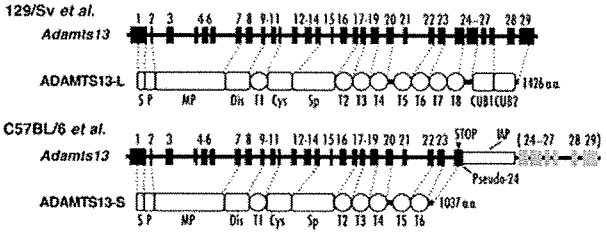

Fig. 1 Gene and protein structure of two kinds of mouse ADAMTS13. In some strains of mice (e.g., C57BL/6), an IAP-retrotransposon (*IAP*) is inserted into intron 23 of the *Adamts13* gene (*arrow*) and creates a pseudo-exon 24 including a premature stop codon. ADAMTS13-S with truncated C-terminal domains is mainly expressed in these strains. *S* Signal peptide, *P* propeptide, *MP* metalloprotease domain, *Dis* disintegrin-like domain, *T* (*numbered 1-8*) thrombospondin type 1 motif domain, *Cys* cysteine-rich domain, *Sp* spacer domain, *CUB* complement components C1r/C1 s, urchin epidermal growth factor, and bone morphogenic protein-1 domain

motif (Tsp1) domains and two CUB domains, designated as ADAMTS13-S, is predominantly expressed in these strains.

Both forms of mouse ADAMTS13 are mainly expressed in the liver and retain a furin-recognition sequence in the propeptide domain, a Zn^{2+}-coordinating active site sequence, the Met residue in a proposed Met-turn, and structural Ca^{2+} coordination residues in the metalloprotease domain, and an RGD sequence in the Cys-rich domain. They show VWF-cleaving activity in vitro but the truncated form exhibits lower activity than the full-length form for purified human VWF multimers [6].

3 Generation of ADAMTS13-deficient mice

Mice deficient in ADAMTS13 have been developed by conventional gene-targeting approaches. Banno et al. generated *Adamts13*$^{-/-}$ mice on a 129/Sv genetic background [2]. Disruption of the gene by replacing exons 3–6, encoding the metalloprotease domain, with a neomycin resistance cassette results in the absence of ADAMTS13 mRNA in liver. ADAMTS13 activity is not detected in plasma of *Adamts13*$^{-/-}$ mice. Analysis of plasma VWF multimer patterns detects UL-VWF multimers in *Adamts13*$^{-/-}$ mice but not in *Adamts13*$^{+/+}$ or *Adamts13*$^{+/-}$ mice, suggesting that the deficiency of ADAMTS13 alone can support the generation of plasma UL-VWF multimers. However, *Adamts13*$^{-/-}$ mice are viable with no apparent signs of TTP. Blood platelet counts, plasma haptoglobin levels and peripheral blood smears are normal in *Adamts13*$^{-/-}$ mice, suggesting a lack of thrombocytopenia and hemolytic anemia. Although pregnancy is a triggering event for TTP, *Adamts13*$^{-/-}$ females survive pregnancy and produce viable offspring of normal-sized litters. Renal histology of pregnant *Adamts13*$^{-/-}$ mice does not show thrombi deposition or excessive VWF accumulation in microvessels.

Motto et al. [3] have generated *Adamts13*$^{-/-}$ mice with elimination of exons 1–6. On a mixed C57BL/6J and 129X1/SvJ genetic background, they are viable without any TTP-like phenotypes, similar to *Adamts13*$^{-/-}$ mice on a 129/Sv genetic background. Thus, both studies clearly indicate that ADAMTS13 deficiency alone is not sufficient to cause TTP-like symptoms in mice. Factors in addition to ADAMTS13 deficiency may be necessary for the development of TTP in mice.

4 The function of ADAMTS13 in thrombosis

4.1 Increased thrombogenesis in ADAMTS13-deficient mice

While *Adamts13*$^{-/-}$ mice do not spontaneously develop TTP, they are in prothrombotic state. Banno et al. revealed that

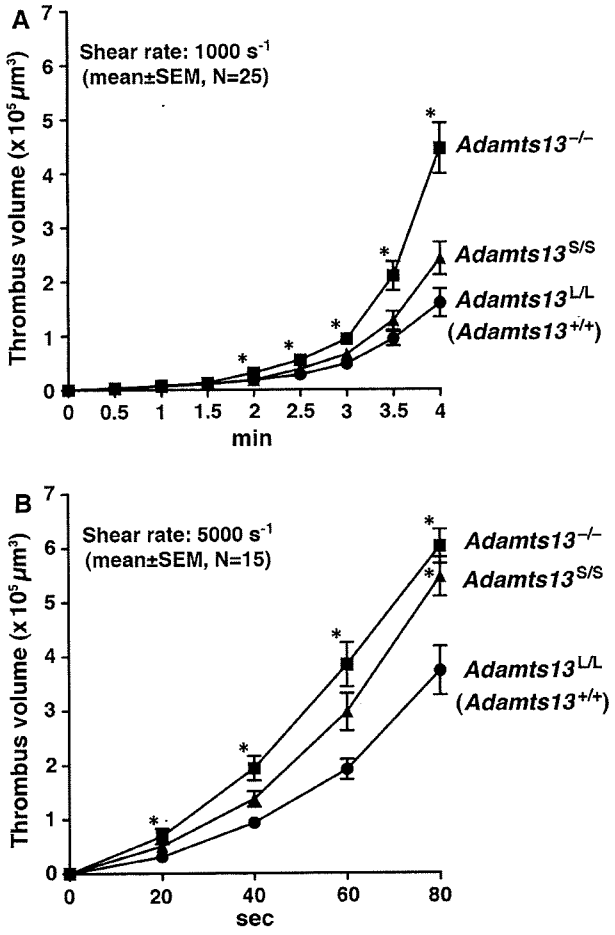

Fig. 2 Platelet thrombus formation in ADAMTS13-mutant mice on collagen surface under flow. **a** Thrombus formation at 1,000 s^{-1}. Whole blood samples from *Adamts13*$^{L/L}$ (*Adamts13*$^{+/+}$), *Adamts13*$^{S/S}$, or *Adamts13*$^{-/-}$ mice containing mepacrine-labeled platelets are perfused over an acid-insoluble type I collagen-coated surface at a wall shear rate of 1,000 s^{-1}. The cumulative thrombus volume, analyzed using a multi-dimensional imaging system, is measured every 0.5 min until 4 min. Data are the mean ± SEM of 25 mice for each genotype. **b** Thrombus formation at 5,000 s^{-1}. Whole blood samples from indicated mice are perfused over an acid-insoluble type I collagen-coated surface at a wall shear rate of 5,000 s^{-1}. The cumulative thrombus volume is measured every 20 s until 80 s. Blood from two mice is pooled and used for experiments. Data are the mean ± SEM of 15 samples for each genotype. *Asterisks* indicate significant differences at $P < 0.05$ in comparison to *Adamts13*$^{L/L}$ mice

accelerated thrombogenic responses in *Adamts13*$^{-/-}$ mice under in vitro flow conditions (Fig. 2). When whole blood is perfused over a collagen-coated surface in a parallel plate-flow chamber at wall shear rates of 750–5,000 s^{-1}, cumulative platelet thrombus volume is significantly higher in *Adamts13*$^{-/-}$ mice compared to *Adamts13*$^{+/+}$ mice [2, 4]. In vivo consequence of a lack of ADAMTS13 was further evaluated using collagen plus epinephrine infusion model experiments. In this model, widespread intravascular thrombosis is induced by intravenous infusion of collagen fibrils in combination with epinephrine, and the incorporation of platelets into thrombi is monitored by the reduction in circulating platelet counts. Following the infusion of collagen plus epinephrine, reduction of platelet counts is more severe in *Adamts13*$^{-/-}$ mice than in *Adamts13*$^{+/+}$ mice, suggesting that a complete lack of ADAMTS13 in mice results in a prothrombotic state.

Using the intravital microscopy, Motto et al. [3] have also elegantly shown prothrombotic phenotypes of *Adamts13*$^{-/-}$ mice in vivo. Upon activation of endothelial cells with secretagogues such as histamine and calcium ionophore A23187, UL-VWF multimers stored in Weibel-Palade bodies are released into circulation. It was demonstrated in vitro that quiescent platelets can rapidly bind to the UL-VWF multimers resulting in formation of long platelet strings and ADAMTS13 can cleave anchored platelet strings on the surface of endothelium [7]. Following stimulation with histamine or A23187, long-lived platelet strings ranging from 30 to 250 μm are observed only in *Adamts13*$^{-/-}$ mice. These strings remain anchored at one end and waved with another end in the blood stream [3]. In addition, following superfusion with A23187, prolonged platelet adhesion is observed in *Adamts13*$^{-/-}$ mice compared to *Adamts13*$^{+/+}$ mice. Adhesion is absent in stimulated veins of *Vwf*$^{-/-}$ mice confirming that prolonged platelet adhesion depends on VWF [3]. These results are the direct evidence that ADAMTS13 regulates VWF-mediated platelet adhesion in vivo.

After topical superfusion of A23187, spontaneous platelet aggregation resulting in microthrombi formation is observed in the microvessels (25–30 μm) of *Adamts13*$^{-/-}$ mice [8]. In *Adamts13*$^{+/+}$ mice treated identically, small platelet aggregates can be seen attached to the endothelium for 1–2 s, but thrombi do not form. When arterioles are injured by a $FeCl_3$-treatment, platelet binding to subendothelium is increased and thrombus formation is significantly accelerated in *Adamts13*$^{-/-}$ mice compared to *Adamts13*$^{+/+}$ mice [8]. In another set of $FeCl_3$-induced vessel injury in *Vwf*$^{-/-}$ mice, most of the vessels do not occlude in either mice expressing ADAMTS13 or lacking ADAMTS13, demonstrating that ADAMTS13 deficiency is not sufficient to overcome the VWF deficiency in this system [9]. These results support that ADAMTS13 down-regulates platelet adhesion and aggregation in vivo, and ADAMTS13 deficiency can provide enhanced thrombus formation at the site of vascular lesions. These findings also suggest that VWF, the only relevant substrate for ADAMTS13, is critical in this model of thrombus growth under arterial shear conditions.

4.2 TTP-like phenotypes induced by shigatoxin challenge in ADAMTS13-deficient mice on the specific genetic background

CASA/Rk strain is a wild-derived mouse strain of *Mus musculus castaneus* that exhibits plasma VWF levels 5- to

10-fold higher than C57BL/6J strain. The major genetic factor that accounts for this difference is associated with a gene modifier *Mvwf2*, corresponding to the R2657Q mutation in *Vwf* gene resulting in increased biosynthesis/secretion of VWF [10]. Additional modifier loci correlating with increased VWF levels are identified in CASA/Rk strain as *Mvwf3* on chromosome 4 and *Mvwf4* on chromosome 13 [10]. The genetic background of CASA/Rk strain has been introduced onto the C57BL/6J and 129/SvJ mixed-background *Adamts13*$^{-/-}$ mice by backcrossing with wild-type CASA mice for two generations. These mice are born in expected Mendelian distribution, however, mean platelet counts of the *Adamts13*$^{-/-}$ mice are significantly reduced compared to *Adamts13*$^{+/+}$ littermates.

When challenged with shigatoxin produced by *Shigella dysenteriae* and the *Shigatoxigenic* group of *Escherichia coli*, a subset of this *Adamts13*$^{-/-}$ mice show clinical signs of TTP including thrombocytopenia, hemolytic anemia with fragmented red blood cells, and VWF-rich thrombi in multiple organs including brain, heart and kidneys [3]. Shigatoxin is toxic to endothelial cells and known to induce hemolytic uremic syndrome (HUS) that exhibits similar clinical and pathologic findings to TTP. Shigatoxin also stimulates the release of UL-VWF multimers from human umbilical vein endothelial cells and perfused quiescent platelets immediately adhere to UL-VWF multimers, resulting in formation of platelet strings [11]. Thus, environmental factors causing endothelial activation or damage can trigger TTP in *Adamts13*$^{-/-}$ mice. Because shigatoxin challenge does not evoke TTP-like symptoms in *Adamts13*$^{-/-}$ mice on the mixed background [3], introduction of the CASA/Rk genetic background provides susceptibility to TTP in *Adamts13*$^{-/-}$ mice. Of note, there is no correlation between plasma VWF level and degree of shigatoxin-induced thrombocytopenia or mortality, suggesting that TTP-modifier genes that are not associated with plasma VWF levels may be delivered from a CASA/Rk genetic background [3].

In human, there is a large variation in the phenotypes of TTP patients with ADAMTS13 deficiency [12]. Many TTP patients with congenital ADAMTS13 deficiency have their first acute episode in the neonatal period or early infancy, but late-onset cases and asymptomatic carriers in adulthood have been reported. Patients with identical ADAMTS13 mutations but different clinical courses have been described, indicating that ADAMTS13 deficiency brings a serious risk but is not a sufficient condition for TTP. Data from *Adamts13*$^{-/-}$ mice support this view, and *Adamts13*$^{-/-}$ mice can contribute to the identification of additional genetic and/or environmental TTP triggers.

The only known substrate for ADAMTS13 is VWF. To investigate the absolute requirement of VWF in shigatoxin-induced thrombocytopenia, VWF-null allele is crossed onto the CASA/*Adamts13*$^{-/-}$ background [9]. Challenge of VWF expressing (*Vwf*$^{+/+}$ or *Vwf*$^{+/-}$) CASA/*Adamts13*$^{-/-}$ mice with shigatoxin results in thrombocytopenia and mortality. In contrast, littermate CASA/*Adamts13*$^{-/-}$ mice deficient for VWF (*Vwf*$^{-/-}$) do not result in thrombocytopenia. These results clearly demonstrate that a threshold of VWF is required for shigatoxin-induced thrombocytopenia and provide experimental evidence for the crucial role of VWF in TTP pathogenesis.

5 Thrombogenic phenotypes in congenic mice having C-terminal truncated ADAMTS13-S

The specific functions of each of the ADAMTS13 domains in the VWF-cleavage have been studied using different types of in vitro assays. These studies have shown an essential role of the N-terminal domains from the metalloprotease to the spacer domains in substrate recognition and proteolysis [1]. However, physiological significance of the remaining C-terminal Tsp1 and CUB domains was not clearly defined in vivo. Taking advantage of the presence of the spontaneous IAP-insertional mutation in the *Adamts13* gene of some laboratory mouse strains, a congenic mouse strain (*Adamts13*$^{S/S}$) that has ADAMTS13-S on 129/Sv genetic background has recently been established [4]. In this model, C57BL/6-*Adamts13* gene with IAP mutation has been applied to 129/Sv mice by ten-generation backcrossing.

Similar to wild-type 129/Sv mice (*Adamts13*$^{L/L}$), *Adamts13*$^{S/S}$ mice do not have UL-VWF multimers in plasma, in contrast to 129/Sv-genetic background ADAMTS13-deficient mice (*Adamts13*$^{-/-}$) [4]. Hence, the C-terminal domains of ADAMTS13 are not necessary for removal of UL-VWF multimers in plasma under physiological conditions. However, parallel plate flow chamber experiments show that blood from *Adamts13*$^{S/S}$ mice is more thrombogenic under flow at a high shear rate of 5,000 s^{-1} in compared to blood from *Adamts13*$^{L/L}$ mice (Fig. 2) [4]. In addition, both in vivo thrombus formation in $FeCl_3$-injured arterioles and thrombocytopenia induced by collagen plus epinephrine challenge are accelerated in *Adamts13*$^{S/S}$ mice compared to *Adamts13*$^{L/L}$ mice [4]. These results provide in vivo insights on physiological significance of the C-terminal domains of ADAMTS13 in down-regulating thrombus growth.

6 The function of ADAMTS13 in sepsis and endotoxemia

Some of the recent studies have found reduced ADAMTS13 activity in patients with acute systemic inflammation

or sepsis, suggesting a role for VWF-ADAMTS13 axis in sepsis [13]. To investigate the functions of VWF and ADAMTS13 in sepsis and endotoxemia, two different groups have done independent studies using two different models; one by LPS-induced sepsis [9] and the other by cecum ligature and puncture (CLP) in mice [14]. When $Vwf^{+/+}$ or $Vwf^{-/-}$ mice are challenged with LPS, there is no significant difference in LPS-induced thrombocytopenia or mortality up to 4 days of observation period [9]. In contrast, in CLP-induced sepsis model there is a decrease in mortality of VWF-deficient mice compared to wild-type mice, suggesting important role for VWF secretion in sepsis-induced mortality [14]. The different finding in two independent studies illustrates the importance of different models used for sepsis.

There is also no significant difference in LPS-induced mortality in VWF expressing mice that are either lacking or expressing ADAMTS13. Additionally, mice deficient for VWF and ADAMTS13 also exhibited similar thrombocytopenia and mortality. These observations in mice suggest that neither absolute VWF deficiency nor ADAMTS13 has effect on LPS-induced sepsis [9]. These findings are in agreement with the report that complete deficiency of ADAMTS13 in mice is not associated with excess mortality in CLP-induced sepsis [14]. However, they have found a decrease in ADAMTS13 activity in wild-type mice after CLP-induced sepsis, similar to that reported previously in human sepsis [13]. However, deficiency of ADAMTS13 in mouse does not modulate CLP-induced sepsis. The decrease in ADAMTS13 activity in CLP-induced sepsis is most probably due to consumption of ADAMTS13 to VWF released in large amounts.

7 The function of ADAMTS13 in inflammation

Recently, Chauhan and colleagues [15] have investigated the role of ADAMTS13 and its substrate VWF in inflammation by studying leukocyte rolling and adhesion in $Adamts13^{+/+}/Vwf^{+/+}$, $Adamts13^{-/-}/Vwf^{+/+}$, $Adamts13^{+/+}/Vwf^{-/-}$ and $Adamts13^{-/-}/Vwf^{-/-}$ mice using intravital microscopy. They have shown that ADAMTS13-deficiency in mice results in higher numbers of leukocytes rolling on the unstimulated endothelium compared to wild-type. The increase in the leukocyte rolling observed in $Adamts13^{-/-}$ mice is VWF-dependent.

There is also an increase in endothelial P-selectin expression, soluble P-selectin and VWF in plasma of $Adamts13^{-/-}$ mice. These observations raise the question how ADAMTS13 deficiency results in increased plasma VWF. One of the reasons could be that ADAMTS13 deficiency results in slower clearance of UL-VWF multimers from the circulation and thus elevated VWF levels.

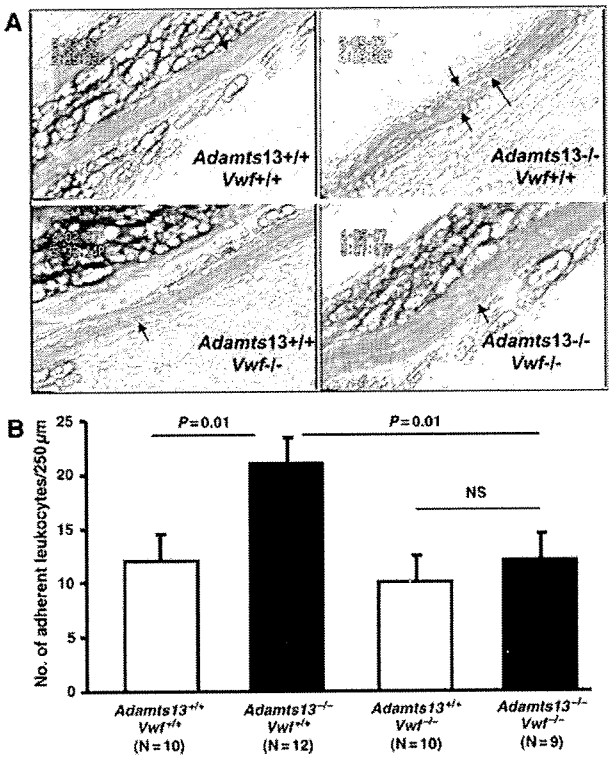

Fig. 3 Increased leukocyte adhesion in the TNF α-stimulated mesenteric venules of ADAMTS13-deficient mice. Mice are treated with the inflammatory cytokine TNF-α for 3.5 h before intravital microscopy. A single mesenteric venule (25–30 µm diameter) is studied per mouse. **a** Representative images are shown. *Arrows* indicate leukocytes adhering to inflamed endothelium. **b** Quantification of the adherent leukocytes. The number of adherent leukocytes is markedly increased in the microvenules of $Adamts13^{-/-}$ mice compared to $Adamts13^{+/+}$ mice. In contrast, the number of leukocytes adhering in venules of $Adamts13^{-/-}/Vwf^{-/-}$ mice is similar to $Adamts13^{+/+}/Vwf^{-/-}$ mice, suggesting that VWF plays a role in increased leukocyte adhesion in $Adamts13^{-/-}$ vessels. Data represent the mean ± SEM. NS, $P > 0.05$

Alternatively, UL-VWF multimers activate platelets, which in turn may activate the endothelium. Previously, it has been shown that activated platelets, by binding to leukocytes, promote Weibel-Palade bodies release and stimulate leukocyte rolling [16]. Interestingly, depletion of platelets in $Adamts13^{-/-}$ mice results in normalization of leukocyte rolling as compared to wild-type mice. This indicates that platelets, likely activated by UL-VWF either in circulation or directly on endothelium, stimulate Weibel-Palade body's secretion. Moreover, when $Adamts13^{-/-}$ mice veins are stimulated with histamine, a secretagogue of Weibel-Palade bodies, in order to release UL-VWF multimers, leukocyte rolling velocity is slower when compared to wild-type mice veins where platelet strings do not form [15]. These in vivo findings are in agreement with previous in vitro studies where it was shown that platelets bound to endothelial UL-VWF could support leukocyte tethering

and rolling and that VWF acts as a ligand for leukocyte receptors PSGL-1 and $\beta 2$ integrin [17].

Inflammatory cytokines TNF-α and IL-8 have been shown to release UL-VWF from human umbilical vein endothelial cells in vitro [18]. When *Adamts13*$^{-/-}$ mice are challenged with TNF-α, the number of adherent leukocytes increases approximately twofold in activated venules of *Adamts13*$^{-/-}$ mice when compared to wild-type mice [15]. This process is dependent on VWF (Fig. 3). In addition, ADAMTS13 deficiency in mouse results in increased extravasation of neutrophils in both thioglycollate-induced peritonitis and wound healing [15]. These in vitro and in vivo studies suggest that UL-VWF multimers released from Weibel-Palade bodies by many stimuli including hypoxia, changes in shear stress, and inflammatory cytokines could accelerate inflammatory responses in diseases such as atherosclerosis and stroke when not digested by ADAMTS13.

The results from the *Adamts13*$^{-/-}$ mice suggest that, by cleaving hyperactive UL-VWF multimers, ADAMTS13 not only down-regulates thrombosis but also inflammation. The studies reported here may provide new insights on the possible uses of ADAMTS13 as a therapeutic agent.

References

1. Banno F, Miyata T. Biology of an antithrombotic factor-ADAMTS13. In: Tanaka K, Davie EW, editors. Recent advances in thrombosis and hemostasis 2008. Springer; 2008. p. 162–76.
2. Banno F, Kokame K, Okuda T, Honda S, Miyata S, Kato H, et al. Complete deficiency in ADAMTS13 is prothrombotic, but it alone is not sufficient to cause thrombotic thrombocytopenic purpura. Blood. 2006;107:3161–6.
3. Motto DG, Chauhan AK, Zhu G, Homeister J, Lamb CB, Desch KC, et al. Shigatoxin triggers thrombotic thrombocytopenic purpura in genetically susceptible ADAMTS13-deficient mice. J Clin Invest. 2005;115:2752–61.
4. Banno F, Chauhan AK, Kokame K, Yang J, Miyata S, Wagner DD, et al. The distal carboxyl-terminal domains of ADAMTS13 are required for regulation of in vivo thrombus formation. Blood. 2009;113:5323–9.
5. Banno F, Kaminaka K, Soejima K, Kokame K, Miyata T. Identification of strain-specific variants of mouse *Adamts13* gene encoding von Willebrand factor-cleaving protease. J Biol Chem. 2004;279:30896–903.
6. Zhou W, Bouhassira EE, Tsai HM. An IAP retrotransposon in the mouse *ADAMTS13* gene creates ADAMTS13 variant proteins that are less effective in cleaving von Willebrand factor multimers. Blood. 2007;110:886–93.
7. Dong JF, Moake JL, Nolasco L, Bernardo A, Arceneaux W, Shrimpton CN, et al. ADAMTS-13 rapidly cleaves newly secreted ultralarge von Willebrand factor multimers on the endothelial surface under flowing conditions. Blood. 2002; 100:4033–9.
8. Chauhan AK, Motto DG, Lamb CB, Bergmeier W, Dockal M, Plaimauer B, et al. Systemic antithrombotic effects of ADAMTS13. J Exp Med. 2006;203:767–76.
9. Chauhan AK, Walsh MT, Zhu G, Ginsburg D, Wagner DD, Motto DG. The combined roles of ADAMTS13 and VWF in murine models of TTP, endotoxemia, and thrombosis. Blood. 2008;111:3452–7.
10. Westrick RJ, Ginsburg D. Modifier genes for disorders of thrombosis and hemostasis. J Thromb Haemost. 2009;7(Suppl 1):132–5.
11. Nolasco LH, Turner NA, Bernardo A, Tao Z, Cleary TG, Dong JF, et al. Hemolytic uremic syndrome-associated Shiga toxins promote endothelial-cell secretion and impair ADAMTS13 cleavage of unusually large von Willebrand factor multimers. Blood. 2005;106:4199–209.
12. Lämmle B, Kremer Hovinga JA, Alberio L. Thrombotic thrombocytopenic purpura. J Thromb Haemost. 2005;3:1663–75.
13. Martin K, Borgel D, Lerolle N, Feys HB, Trinquart L, Vanhoorelbeke K, et al. Decreased ADAMTS-13 (A disintegrin-like and metalloprotease with thrombospondin type 1 repeats) is associated with a poor prognosis in sepsis-induced organ failure. Crit Care Med. 2007;35:2375–82.
14. Lerolle N, Dunois-Larde C, Badirou I, Motto DG, Hill G, Bruneval P, et al. von Willebrand factor is a major determinant of ADAMTS-13 decrease during mouse sepsis induced by cecum ligation and puncture. J Thromb Haemost. 2009;7:843–50.
15. Chauhan AK, Kisucka J, Brill A, Walsh MT, Scheiflinger F, Wagner DD. ADAMTS13: a new link between thrombosis and inflammation. J Exp Med. 2008;205:2065–74.
16. Dole VS, Bergmeier W, Mitchell HA, Eichenberger SC, Wagner DD. Activated platelets induce Weibel-Palade-body secretion and leukocyte rolling in vivo: role of P-selectin. Blood. 2005; 106:2334–9.
17. Pendu R, Terraube V, Christophe OD, Gahmberg CG, de Groot PG, Lenting PJ, et al. P-selectin glycoprotein ligand 1 and beta2-integrins cooperate in the adhesion of leukocytes to von Willebrand factor. Blood. 2006;108:3746–52.
18. Bernardo A, Ball C, Nolasco L, Moake JF, Dong JF. Effects of inflammatory cytokines on the release and cleavage of the endothelial cell-derived ultralarge von Willebrand factor multimers under flow. Blood. 2004;104:100–6.

Journal of the American College of Cardiology
© 2009 by the American College of Cardiology Foundation
Published by Elsevier Inc.

Vol. 53, No. 8, 2009
ISSN 0735-1097/09/$36.00
doi:10.1016/j.jacc.2008.11.014

PRE-CLINICAL RESEARCH

Prolonged Targeting of Ischemic/Reperfused Myocardium by Liposomal Adenosine Augments Cardioprotection in Rats

Hiroyuki Takahama, MD,*†‡ Tetsuo Minamino, MD, PHD,§ Hiroshi Asanuma, MD, PHD,† Masashi Fujita, MD, PHD,§ Tomohiro Asai, PHD,¶ Masakatsu Wakeno, MD, PHD,*†‡ Hideyuki Sasaki, MD,*†‡ Hiroshi Kikuchi, PHD,# Kouichi Hashimoto,** Naoto Oku, PHD,¶ Masanori Asakura, MD, PHD,† Jiyoong Kim, MD,† Seiji Takashima, MD, PHD,§ Kazuo Komamura, MD, PHD,|| Masaru Sugimachi, MD, PHD,|| Naoki Mochizuki, MD, PHD,*‡ Masafumi Kitakaze, MD, PHD, FACC†

Osaka, Shizuoka, and Tokyo, Japan

Objectives The purpose of this study was to investigate whether liposomal adenosine has stronger cardioprotective effects and fewer side effects than free adenosine.

Background Liposomes are nanoparticles that can deliver various agents to target tissues and delay degradation of these agents. Liposomes coated with polyethylene glycol (PEG) prolong the residence time of drugs in the blood. Although adenosine reduces the myocardial infarct (MI) size in clinical trials, it also causes hypotension and bradycardia.

Methods We prepared PEGylated liposomal adenosine (mean diameter 134 ± 21 nm) by the hydration method. In rats, we evaluated the myocardial accumulation of liposomes and MI size at 3 h after 30 min of ischemia followed by reperfusion.

Results The electron microscopy and ex vivo bioluminescence imaging showed the specific accumulation of liposomes in ischemic/reperfused myocardium. Investigation of radioisotope-labeled adenosine encapsulated in PEGylated liposomes revealed a prolonged blood residence time. An intravenous infusion of PEGylated liposomal adenosine (450 μg/kg/min) had a weaker effect on blood pressure and heart rate than the corresponding dose of free adenosine. An intravenous infusion of PEGylated liposomal adenosine (450 μg/kg/min) for 10 min from 5 min before the onset of reperfusion significantly reduced MI size (29.5 ± 6.5%) compared with an infusion of saline (53.2 ± 3.5%, $p < 0.05$). The antagonist of adenosine A_1, A_{2a}, A_{2b}, or A_3 subtype receptor blocked cardioprotection observed in the PEGylated liposomal adenosine-treated group.

Conclusions An infusion as PEGylated liposomes augmented the cardioprotective effects of adenosine against ischemia/reperfusion injury and reduced its unfavorable hemodynamic effects. Liposomes are promising for developing new treatments for acute MI. (J Am Coll Cardiol 2009;53:709–17) © 2009 by the American College of Cardiology Foundation

Liposomes are now widely used for drug delivery in cancer treatment to target specific organs actively or passively and to prevent the degradation of chemotherapy agents (1). However, the application of liposomes for cardiovascular diseases is still limited. In ischemic/reperfused myocardium, cellular permeability is enhanced and vascular endothelial integrity is disrupted (2,3), suggesting that nanoparticles

See page 718

*From the Department of Molecular Imaging in Cardiovascular Medicine, Osaka University Graduate School of Medicine, Osaka, Japan; †Department of Cardiovascular Medicine, National Cardiovascular Center, Osaka, Japan; ‡Department of Structural Analysis, Research Institute, National Cardiovascular Center, Osaka, Japan; §Department of Cardiovascular Medicine, Osaka University Graduate School of Medicine, Osaka, Japan; ||Department of Cardiovascular Dynamics, Research Institute, National Cardiovascular Center, Osaka, Japan; ¶Department of Medical Biochemistry, School of Pharmaceutical Sciences, University of Shizuoka, Shizuoka, Japan; #Daiichi Pharmaceutical Co., Tokyo, Japan; and the **Daiichi-Sankyo Pharmaceutical Co., Tokyo, Japan. Supported by a grant for Scientific Research and a grant for the Advancement of Medical Equipment from the Japanese Ministry of Health, Labor, and Welfare, as well as a grant from the Japan Cardiovascular Research Foundation.

Manuscript received September 4, 2008; revised manuscript received October 21, 2008, accepted November 3, 2008.

Abbreviations and Acronyms

8-SPT = 8-(p-sulfophenyl) theophylline
EM = electron microscopy
MI = myocardial infarction
PEG = polyethylene glycol
RI = radioisotope
TTC = triphenyltetrazolium chloride

such as liposomes may be a promising drug delivery system for targeting damaged myocardium with cardioprotective agents. Additionally, coating liposomes with polyethylene glycol (PEG) prolongs their residence time in the circulation (1). Because enhanced microvascular permeability persists for at least 48 h after the occurrence of myocardial infarction (MI) (2), drugs delivered in PEGylated liposomes should be able to display their maximum beneficial effects on myocardial damage after MI.

Adenosine has multiple physiological functions that are mediated via the adenosine A_1, A_{2a}, A_{2b}, and A_3 receptors (4,5). Although large-scale clinical trials suggested the potential value of adenosine therapy for patients with acute MI (6,7), this agent has an extremely short half-life (1 to 2 s) and causes hypotension and bradycardia because of vasodilatory and negative chronotropic effects (4). Because a high dose of adenosine is required to exert cardioprotective effects, it is difficult to use clinically because of the associated hemodynamic consequences. Therefore, we hypothesized that adenosine encapsulated in PEGylated liposomes would cause less hemodynamic disturbance and might also specifically accumulate in ischemic/reperfused myocardium, leading to augmented cardioprotective effects. To test this hypothesis, we created PEGylated liposomal adenosine by the hydration method and investigated: 1) whether liposomal adenosine accumulated in ischemic/reperfused myocardium and prolonged blood residence time; 2) whether liposomal adenosine caused less severe hypotension and bradycardia than free adenosine; and 3) which adenosine receptor subtype was involved in mediating the cardioprotective effects of liposomal adenosine against ischemia/reperfusion injury.

Methods

Materials. The materials for preparing PEGylated liposomes, including hydrogenated soy phosphatidyl choline (HSPC), 1,2-distearoyl-sn-glycero-3-phosphoethanolamine-n-[methoxy (polyethylene glycol)-2000] (DSPE-PEG2000), and cholesterol were obtained from Nissei Oil Co., Ltd. (Tokyo, Japan) and Wako Pure Chemical Co., Ltd. (Osaka, Japan). [^{3}H]-adenosine was purchased from Daiichi Pure Chemicals Co., Ltd. (Tokyo, Japan). Other materials were obtained from Sigma (St. Louis, Missouri), including 8-(*p*-sulfophenyl)theophylline (8-SPT; a nonselective adenosine receptor antagonist), 1,3-diethyl-8-phenylxanthine (DPCPX; a selective adenosine A_1 receptor antagonist), 5-amino-7-(phenylethyl)-2-(2-furyl)-pyrazolo[4,3-e]-1,2,4-triazolo[1,5-c] pyrimidine (SCH58261; a selective adenosine A_{2a} receptor antagonist), 8-[4-[((4-cyanophenyl)carbamoylmethyl) oxy]phenyl]-1, 3-di(n-propyl)xanthine (MRS1754; a selective adenosine A_{2b} receptor antagonist), and 5-propyl-2-ethyl-4-propyl-3-(ethylsulfanylcarbonyl)-6-phenylpyridine-5-carboxylate (MRS1523, a selective adenosine A_3 receptor antagonist).

Animals. Male Wistar rats (9 weeks old and weighing 250 to 310 g, Japan Animals, Osaka, Japan) were used. The animal experiments were approved by the National Cardiovascular Center Research Committee and were performed according to institutional guidelines.

Preparation of PEGylated liposomes. The PEGylated liposomes were prepared by the hydration method. Briefly, adenosine was added to the lipid solution. After mixture of lipid and adenosine, DSPE-PEG2000 was added and incubated. The final composition of PEGylated liposomes was HSPC:cholesterol:DSPE-PEG2000 = 6.0:4.0:0.3 (molar ratio). After ultracentrifugation several times, the pellet of liposomal adenosine was resuspended in sodium lactate at each required concentration for use in the experimental protocols. Some samples of final liposomal adenosine were disrupted by dilution with 50% methanol (1.5 ml per 30-μl of liposomes). After 10 min of ultracentrifugation, the concentration of adenosine in the supernatant was measured by high-performance liquid chromatography.

To prepare fluorescent-labeled liposomes, 0.5 mol% tetramethylrhodamine isothiocyanate (rhodamine) was added to the lipid mixture. To prepare radioisotope (RI)-labeled adenosine encapsulated in liposomes, [^{3}H]-radiolabeled adenosine (Daiichi Pure Chemicals, Tokyo, Japan) was diluted with free adenosine and was encapsulated in liposomes as described above.

Characterization of PEGylated liposomal adenosine. The characterization of the liposomes was performed by the dynamic scatter analysis (Zetasizer Nano ZS, Malvern, Worcestershire, United Kingdom). The analyses were performed 10 times per sample, and results represented analyses of 4 independent experiments.

Experimental protocols. PROTOCOL 1: EFFECTS OF PEGYLATED LIPOSOMAL ADENOSINE ON HEMODYNAMICS IN RATS. Rats were anesthetized with intraperitoneal sodium pentobarbital (50 mg/kg). Catheters were advanced into a femoral artery and vein for the measurement of systemic blood pressure and infusion of drugs, respectively. Both blood pressure and heart rate were monitored continuously during the study using a Power Lab (AD Instruments, Castle Hill, Australia). After hemodynamics became stable, we intravenously administered empty PEGylated liposomes (n = 8), free adenosine (n = 8), or PEGylated liposomal adenosine (n = 8) for 10 min. Either PEGylated liposomal or free adenosine was infused at an initial dose of 225 μg/kg/min (0.1 ml/min) for 10 min. After a 5-min interval, either PEGylated liposomal adenosine or free adenosine was infused at 450 μg/kg/min (0.1 ml/min) for 10 min. In the same manner, PEGylated liposomal adenosine or free adenosine was then infused at 900 μg/kg/min (0.1 ml/min).

PROTOCOL 2: EFFECTS OF PEGYLATED LIPOSOMAL ADENOSINE ON INFARCT SIZE IN RATS. The MI was induced by transient ligation of the left coronary artery as described previously (8). In the first series of experiments, to examine the dose-dependent effects of liposomal adenosine on MI size, PEGylated liposomal adenosine was infused intravenously at 50, 150, or 450 μg/kg/min for a 10-min period starting from 5 min before the onset of reperfusion. In the second series of experiments, to determine the adenosine receptor subtype involved in cardioprotective effects by the liposomal adenosine, the antagonist of adenosine subtype receptor was intravenously injected as a bolus followed by the infusion of liposomal adenosine for 10 min. The MI size was evaluated at 3 h after the start of reperfusion. The doses of adenosine receptor subtype antagonists were determined according to the previous reports (9–11).

Measurement of infarct size. At 3 h after the onset of reperfusion, the area at risk and the infarcted area were determined by Evans blue and triphenyltetrazolium chloride (TTC) staining, respectively, as previously described (8). Infarct size was calculated as [infarcted area/area at risk] × 100(%) in a blind manner. The area at risk was composed of border (TTC staining) and infarcted (TTC nonstaining) areas.

Electron microscopy (EM). Myocardial samples for EM were obtained from the central and peripheral areas in ischemic/reperfused myocardium, which roughly corresponded to the infarcted and border areas, respectively, after the left coronary artery was occluded for 30 min of ischemia followed by 3 h of reperfusion. Samples were prepared as previously reported (12). Liposomes, whose major membrane component is unsaturated phospholipids, were visualized as homogenous dark dots with a diameter of 100 to 150 nm (13).

Accumulation of fluorescent-labeled PEGylated liposomes in ischemic/reperfused myocardium. Unlabeled or fluorescent-labeled PEGylated liposomes were infused intravenously at a dose of 0.1 ml/min as liposomal adenosine was infused in protocol 2. At 3 h after reperfusion, hearts were quickly removed and cut into 4 sections parallel to the axis from base to apex. Then ex vivo bioluminescence imaging was performed with an Olympus OV 100 imaging system (Olympus, Tokyo, Japan) and signals were quantified using WASABI quantitative software (Hamamatsu Photonics K.K., Shizuoka, Japan). Fluorescent intensity in the region of interest was measured as previously reported (14). Control intensity indicated the fluorescent intensity in the nonischemic area of the individual rat.

Time-course changes of free and PEGylated liposomal RI-labeled adenosine in plasma and myocardium. Free or PEGylated liposomal [^{3}H]-adenosine (83 kBq per rat) was infused intravenously at a dose of 0.1 ml/min as liposomal adenosine was infused in protocol 2. At the time indicated, rat hearts were harvested for counting of radioactivity (LSC-3100, Aloka Co., Tokyo, Japan). Results are expressed as a percentage of the injected dose per 1 ml of blood or 1 g of wet tissue weight.

Statistical analysis. The parameters of the liposomes were expressed as the average ± SD, whereas other data were expressed as the average ± SEM. Comparison of time-course changes in hemodynamic parameters between groups was performed by 2-way repeated-measures analysis of variance (ANOVA) followed by a post-hoc Bonferroni test. For comparison of RI activity between groups, statistical analysis was done with the Mann-Whitney *U* test. To address the differences in infarct size among groups, we performed a nonparametric (Kruskal-Wallis) test followed by evaluation with the Mann-Whitney *U* test. Resulting p values were corrected according to the Bonferroni method. To compare parameters of liposomes, an unpaired *t* test was performed. In all analyses, $p < 0.05$ was considered to indicate statistical significance.

Results

Characterization of liposomes by dynamic light scatter analysis. The dynamic light scatter analysis showed no significant difference in mean diameter, polydispersity index, or zeta-potential distribution between empty and adenosine-loaded PEGylated liposomes (Table 1).

Liposomes in ischemic/reperfused myocardium. The EM revealed the intact vascular endothelial cells and cardiomyocytes in the nonischemic myocardium (Figs. 1A and 1B). There were no homogenous dark dots indicating liposomes in the nonischemic myocardium of rats that received either saline (Fig. 1A) or liposomes (Fig. 1B). In the border area, many homogenous dark dots indicating liposomes were accumulated in rats that received liposomes, but not saline (Figs. 1C and 1D). In this area, significant structural damage was not observed in endothelium, but slight swelling of mitochondria was often observed. In the infarcted area, numerous liposomes were detected in rats that received liposomes, but not saline (Figs. 1E and 1F). In this area, the disrupted endothelial integrity and marked swelling of mitochondria were often observed.

Table 1 Characterization of Liposomes by Dynamic Light Scatter Analysis

	Mean Diameter (nm)	Polydispersity Index	Zeta Potential (mV)
PEGylated liposomes (empty liposomes)	126 ± 12	0.035 ± 0.003	−1.7 ± 0.4
PEGylated liposomal adenosine	134 ± 21	0.094 ± 0.002	−2.3 ± 1.1

Results represented analysis of 4 independent experiments. Values are expressed as mean ± SD.
PEG = polyethylene glycol.

JACC Vol. 53, No. 8, 2009
February 24, 2009:709–17

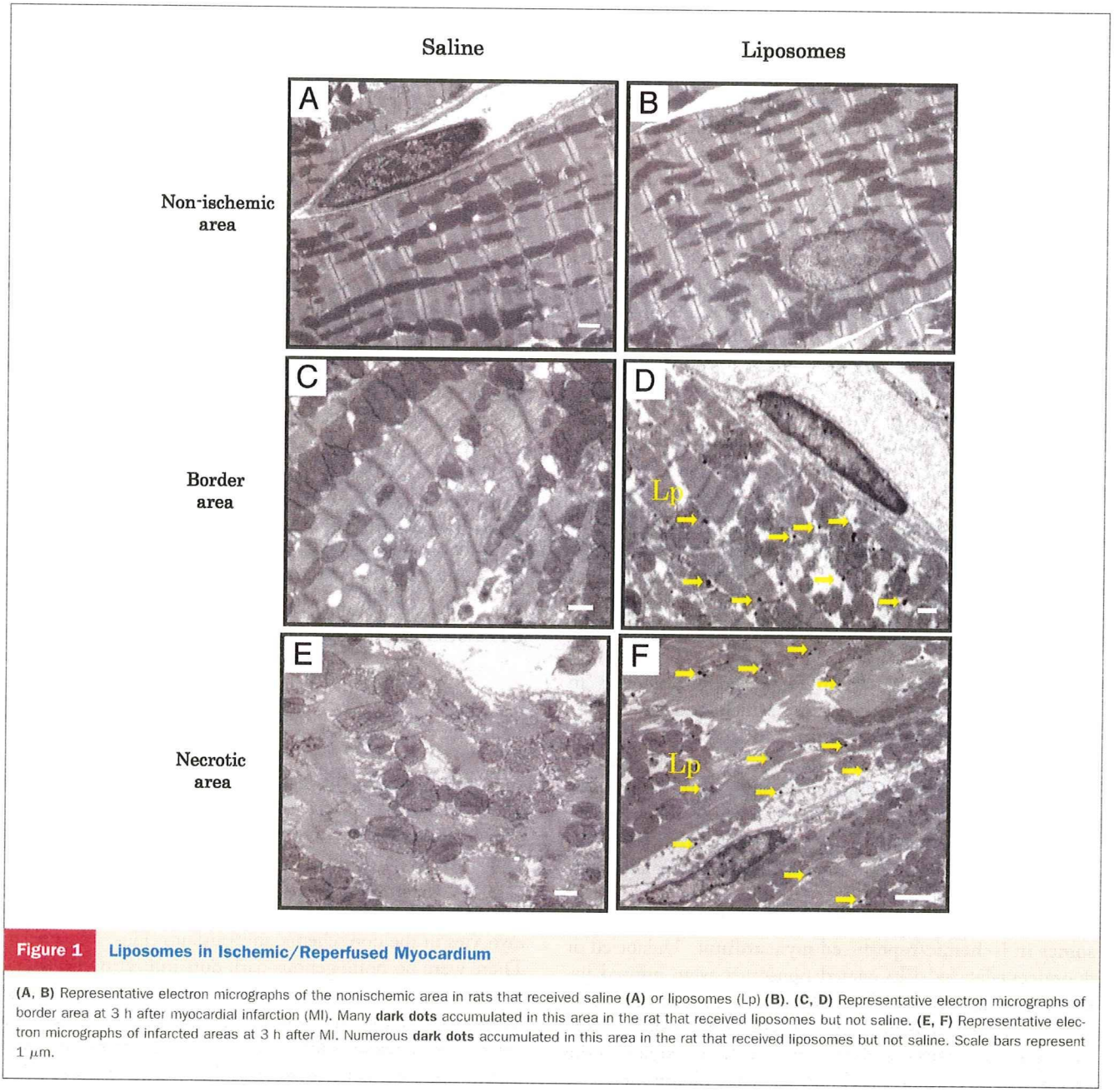

Figure 1 Liposomes in Ischemic/Reperfused Myocardium

(A, B) Representative electron micrographs of the nonischemic area in rats that received saline **(A)** or liposomes (Lp) **(B)**. **(C, D)** Representative electron micrographs of border area at 3 h after myocardial infarction (MI). Many **dark dots** accumulated in this area in the rat that received liposomes but not saline. **(E, F)** Representative electron micrographs of infarcted areas at 3 h after MI. Numerous **dark dots** accumulated in this area in the rat that received liposomes but not saline. Scale bars represent 1 μm.

Fluorescent-labeled PEGylated liposomes in ischemic/reperfused myocardium. Quantitative analysis by bioluminescence ex vivo bioluminescene imaging revealed that the target to control fluorescent intensity ratio was higher in the border (noninfarcted area at risk) as well as infarcted areas compared with a nonischemic one, suggesting that fluorescent-labeled liposomes were accumulated in the border as well as infarcted areas. Since there was no high-intensity area when unlabeled liposomes were infused, it was suggested that this was not a nonspecific phenomenon to MI by the ex vivo bioluminescence imaging system (Fig. 2). The Evans blue staining was unrelated to the fluorescence intensity (data not shown).

Plasma radioactivity of RI-labeled adenosine was markedly higher in the PEGylated liposomal adenosine group at 10 min and 3 h after the intravenous infusion than in the free adenosine group (Fig. 3A). Encapsulation within PEGylated liposomes also augmented the accumulation of adenosine in ischemic/reperfused myocardium compared with that of free adenosine (Fig. 3B).

Hemodynamic effects of PEGylated liposomal adenosine. Baseline hemodynamic parameters did not differ among the groups. An intravenous infusion of free adenosine at doses of 225, 450, and 900 μg/kg/min decreased the mean blood pressure by 14.8%, 25.4%, and 33.7%, respectively, compared with the effect of empty PEGylated lipo-

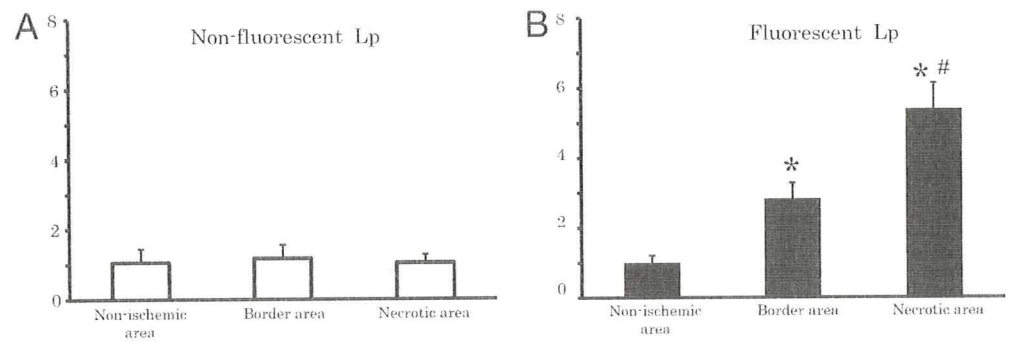

Figure 2 Detection of Fluorescence-Labeled PEGylated Liposomes in Ischemic/Reperfused Myocardium

Quantitative analysis of target-to-control fluorescent intensity ratio for each area in rats (n = 3 each group) that received nonfluorescent **(A)** or fluorescent **(B)** liposomes. The values of bioluminescence signals in the border and infarcted areas were expressed as the fold to that of the each nonischemic area. Values are expressed as the mean ± SEM (error bars). *p < 0.05 versus nonischemic areas. #p < 0.05 versus border areas.

somes. In contrast, the intravenous infusion of PEGylated liposomal adenosine at a dose of either 225 or 450 μg/kg/min did not significantly alter mean blood pressure (Fig. 4). Changes of the heart rate after infusion of PEGylated liposomal adenosine or free adenosine were similar to those observed for mean blood pressure (Fig. 4).

Effects of PEGylated liposomal adenosine on MI size. Baseline hemodynamic parameters were similar among all of the groups (Table 2). Intravenous infusion of free adenosine for 10 min reduced both the blood pressure and the heart rate, although these parameters returned to baseline within 5 min of ceasing infusion (Table 2). In contrast, hemodynamic parameters of the other groups were not altered (Table 2). The area at risk in the control group (61 ± 3%) did not differ compared with those of other groups that received liposomal adenosine. Intravenous infusion of PEGylated liposomal adenosine caused a dose-dependent decrease of MI size compared with that in the control group, whereas intravenous infusion of empty PEGylated liposomes or free adenosine did not (Fig. 5B).

The bolus injection of adenosine receptor antagonist did not alter the hemodynamic parameters (Table 3). The area at risk in the liposomal adenosine group (58 ± 3%) did not differ compared with those of other groups that received adenosine receptor antagonist. Infusion of 8-SPT, a nonspecific adenosine receptor antagonist, blunted the cardioprotective effect of liposomal adenosine (Fig. 6B). Furthermore, the infusion of the adenosine A_1, A_{2a}, A_{2b}, or A_3 receptor antagonist also blunted cardioprotective effects of liposomal adenosine (Fig. 6B). Infusion of 8-SPT alone did not significantly affect myocardial infarct size compared with the control (52 ± 5%, n = 4).

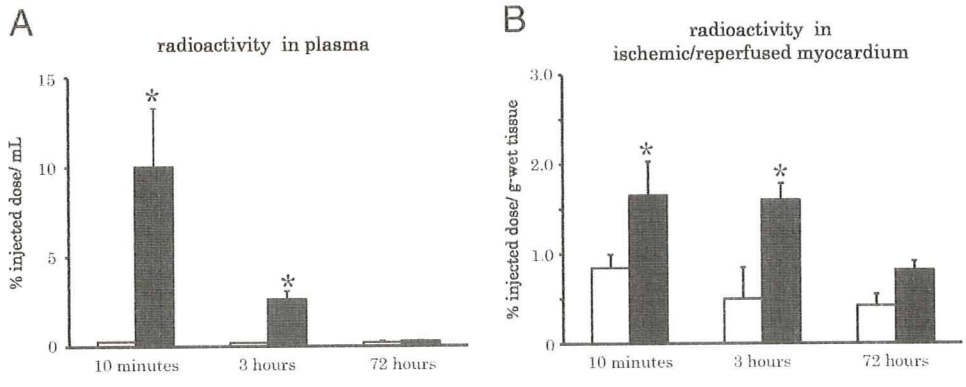

Figure 3 Radioisotope-Labeled Adenosine in Plasma and Ischemic/Reperfused Myocardium

(A) Changes in plasma radioactivity after infusion of radioisotope-labeled adenosine. **Solid and open bars** indicate the PEGylated liposomal adenosine and free adenosine groups, respectively (n = 4 each). In the PEGylated liposomal adenosine group, plasma radioactivity was markedly higher than in the free adenosine group. **(B)** Changes in radioactivity in ischemic/reperfused myocardium. **Solid and open bars** indicate the PEGylated liposomal adenosine and free adenosine groups, respectively (n = 4 each). In the PEGylated liposomal adenosine group, myocardial radioactivity was markedly higher than in the free adenosine group. Values are expressed as the mean ± SEM (error bars). *p < 0.05 versus the free adenosine group at the corresponding time.

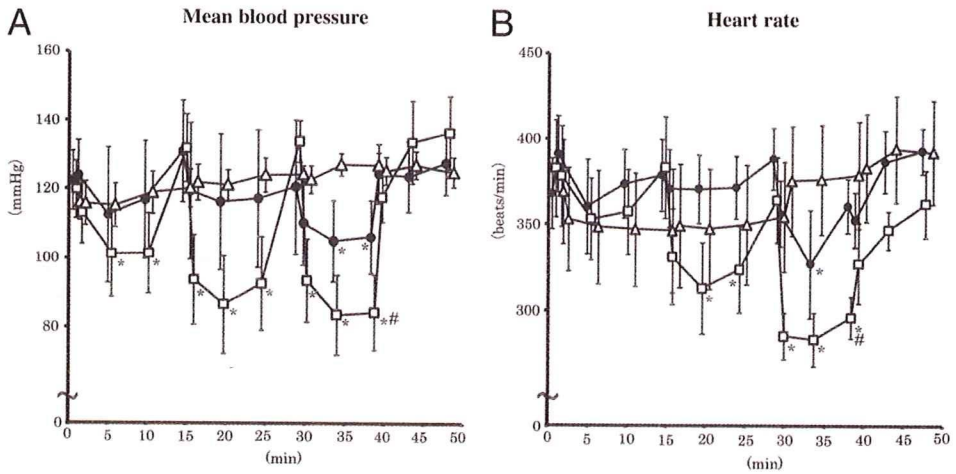

Figure 4 Hemodynamic Effects of PEGylated Liposomal Adenosine

Changes in the mean blood pressure **(A)** and heart rate **(B)** after intravenous infusion of various doses of empty PEGylated liposomes **(triangles)**, PEGylated liposomal adenosine **(circles)**, or free adenosine **(squares)** (n = 8 each). Values are expressed as the mean ± SEM. *p < 0.05 versus baseline at the corresponding group. #p < 0.05 versus PEGylated liposomes.

Discussion

In the present study, EM, bioluminescence ex vivo imaging, and fluorescent analysis revealed the accumulation of liposomes in the border (noninfarcted areas at risk) as well as infarcted ones, but not nonischemic myocardium, at 3 h after MI. These findings suggested that liposomes could specifically accumulate in ischemic/reperfused myocardium. Interestingly, EM revealed the existence of liposomes at sites where endothelial integrity was still morphologically maintained. Endothelial dysfunction such as enhanced permeability is induced by ischemic insult without morphological endothelial disruption (3,15). Enhanced permeability might lead to the accumulation of liposomes in the border as well as infarcted area, which will contribute to salvage the ischemic/reperfused myocardium. However, further investigation will be needed to determine the precise mechanism by which liposomes accumulate in ischemic/reperfused myocardium.

Analysis using RI-labeled adenosine encapsulated in liposomes revealed that plasma radioactivity was markedly higher in the PEGylated liposomal adenosine group compared with the free adenosine group. This indicates that encapsulation of adenosine by PEGylated liposomes considerably prolonged its residence time in the circulation and delayed its degradation. Consistent with the histological data, RI-labeled adenosine also showed preferential accumulation in ischemic/reperfused myocardium.

Table 2 Effects of Liposomal Adenosine on Hemodynamic Parameters

		Ischemia				Reperfusion	
	Baseline	0 min	15 min	25 min	30 min	5 min	10 min
Mean blood pressure (mm Hg)							
Saline	122 ± 5	102 ± 10	108 ± 7	107 ± 9	108 ± 7	105 ± 9	104 ± 9
Vehicle	127 ± 4	109 ± 8	108 ± 7	111 ± 9	111 ± 5	105 ± 5	103 ± 5
Free-Ado	124 ± 8	115 ± 8	111 ± 5	109 ± 4	66 ± 4*	62 ± 4*	112 ± 6
Lp-Ado 50 μg/kg/min	121 ± 5	106 ± 6	105 ± 6	110 ± 10	102 ± 6	101 ± 6	104 ± 4
Lp-Ado 150 μg/kg/min	122 ± 3	107 ± 6	107 ± 6	109 ± 11	105 ± 6	100 ± 6	103 ± 4
Lp-Ado 450 μg/kg/min	124 ± 3	104 ± 6	105 ± 6	107 ± 5	102 ± 6	99 ± 6	104 ± 4
Heart rate (beats/min)							
Saline	363 ± 22	366 ± 19	369 ± 14	413 ± 22	372 ± 12	372 ± 16	371 ± 14
Vehicle	363 ± 32	363 ± 6	383 ± 6	396 ± 25	367 ± 6	374 ± 7	372 ± 7
Free-Ado	360 ± 18	361 ± 17	384 ± 13	379 ± 18	305 ± 11*	293 ± 13*	356 ± 14
Lp-Ado 50 μg/kg/min	378 ± 19	386 ± 21	366 ± 12	376 ± 12	367 ± 19	369 ± 9	377 ± 17
Lp-Ado 150 μg/kg/min	388 ± 27	376 ± 20	371 ± 14	377 ± 13	378 ± 16	373 ± 16	369 ± 17
Lp-Ado 450 μg/kg/min	368 ± 17	376 ± 21	361 ± 13	386 ± 15	368 ± 15	363 ± 6	367 ± 7

Values are expressed as mean ± SEM. *p < 0.05 versus baseline.
Free-Ado = free adenosine; Lp-Ado = PEGylated liposomal adenosine; PEG = polyethylene glycol; vehicle = PEGylated liposomes.